The Slow Sea Surface Temperature Mode and the Fast-Wave Limit: Analytic Theory for Tropical Interannual Oscillations and Experiments in a Hybrid Coupled Model

J. DAVID NEELIN

Department of Atmospheric Sciences, University of California at Los Angeles, Los Angeles, California

(Manuscript received 19 January 1990, in final form 14 September 1990)

ABSTRACT

A modified shallow water model with simplified mixed layer dynamics and a sea surface temperature (SST) equation is employed to gain a theoretical understanding of the modes and mechanisms of coupled air–sea interaction in the tropics. Approximations suggested by a scaling analysis are used to obtain analytic results for the eigenmodes of the system. A slow time scale, unstable eigenmode associated with the time derivative of the SST equation is suggested to be important in giving rise to interannual oscillations. This slow SST mode is not necessarily linked to conventional equatorial oceanic wave modes. A useful limit of this mode is explored in which the wave speed of uncoupled oceanic wave modes is fast compared to the time scales that arise from the coupling. This is referred to as the fast-wave limit. The dispersion relationship in this limit is used to present a number of coupled feedback mechanisms, which contribute simultaneously to the instability of the SST mode.

It is suggested that interannual oscillations observed in a hybrid coupled general circulation model (HGCM) are related to the slow SST mode. A method of testing applicability of the fast-wave limit in any coupled model through distorted physics experiments is presented. Such experiments with the HGCM are employed to demonstrate that the fast-wave limit is quite a good approximation for interannual oscillations at moderate coupling. It is shown that the time delay associated with oceanic wave propagation across the basin is not essential to the existence of interannual coupled oscillations.

Asymptotic expressions are also derived for the eigenvalues of coupled Rossby and Kelvin wave modes in the simple model. The manner in which various coupling mechanisms affect the stability of these modes is discussed and the results are used to explain the behavior of a secondary bifurcation found in the HGCM in terms of coupled Kelvin wave instability. For coupled Rossby and Kelvin modes, various coupling mechanisms oppose one another, suggesting that instability of these modes will be less robust to changes of model parameters and basic state than that of the SST mode, in which all coupling mechanisms tend to give growth.

1. Introduction

The interpretation of behavior found by numerical integration in a general circulation model (GCM) always presents difficulties due to the number and complexity of the processes involved. The approach taken here is to construct the minimum model with which some theoretical understanding may be gained of the phenomena observed in more complicated coupled models. Pioneering studies of El Niño, such as Cane and Zebiak (1985), Zebiak and Cane (1987), Schopf and Suarez (1988), Philander et al. (1984) and Hirst (1988), have been carried out with modified shallow water models and so a model of this class is employed. Because the space of potentially important parameters is fairly large even in this simplified model, analytic results are preferred over numerical ones and the model is constructed and scaled in such a way as to permit this. In particular, some degree of independence from the exact formulation of the atmospheric model is sought, albeit at the expense of some idealization.

The analytic, asymptotic results obtained from the simple model depend on a number of assumptions, not all of which will necessarily hold in a coupled system of full complexity. They are presented to provide a conceptual framework in which to discuss the mechanisms contributing to interannual oscillations. As a concrete demonstration of their utility, they are applied to understanding the results of a more complex model. This other model is a hybrid coupled general circulation model for El Niño studies, described in Neelin (1990, N hereafter). The model consists of an ocean general circulation model in an idealized Pacific Ocean basin, coupled to a two-level, steady-state atmospheric model with parameterized moist processes. The combination of an ocean GCM with a simpler steady atmospheric model is referred to as a hybrid coupled GCM or HGCM. The choice of coupling to a steady atmospheric model permits the examination of a deterministic coupled system unperturbed by atmospheric variability, which nonetheless has the full nonlinearity of an ocean

Corresponding author address: Dr. J. David Neelin, Department of Atmospheric Sciences, UCLA, 405 Hilgard Avenue, Los Angeles, CA 90024.

GCM. As described in N, interannual oscillations are found in the HGCM which resemble the El Niño–Southern oscillation (ENSO) cycle in a number of ways. Equatorially trapped coupled oscillations of three to four year period arise as a Hopf bifurcation as parameters affecting the coupling or the climatology are changed. Factors tending to favor instability include a reduction of the climatological upwelling, an increase of the atmospheric model wind stress response to sea surface temperature (SST) anomalies or an increase in the near-surface vertical temperature gradient along the equator. At higher coupling, a secondary bifurcation occurs, giving rise to additional five to six month oscillations which complicate the time evolution of the coupled system. The results from the simple model are employed to explain the mechanisms giving rise to these bifurcations.

A question of importance to tropical coupled modeling is whether the lag time associated with uncoupled oceanic mode transit times across the basin is essential to interannual coupled oscillations. This hypothesis was formulated as a simple delayed oscillator model by Schopf and Suarez (1987) to provide an analog to modified shallow water model results. A similar model in a slightly different parameter range has been shown by Battisti and Hirst (1988) to account reasonably well for the oscillation found in the Cane and Zebiak model. The simple model presented here is employed to suggest that in some parameter regimes, the wave transit time is *not* important, and a useful idealization of a mode independent from the oceanic wave modes is given. Perhaps most importantly, a distorted physics method for testing these theoretical results in any primitive equation or shallow water model is put forward. Such distorted physics experiments are presented with the primitive-equation HGCM to obtain definitive results on the question of whether wave time scales are essential to the existence of interannual oscillations.

The simple model is presented in section 2 and a scaling analysis is carried out in section 3 to suggest small parameters that may be useful in generating approximations. A case of particular note is referred to as the "fast-wave" limit, since it occurs when the equatorial wave speed is sufficiently fast compared to time scales of advection and coupling that the ocean comes into dynamic adjustment quickly compared to the effects of coupling. In section 4, asymptotic results for eigenvalues are obtained by an expansion in small parameters both for coupled Kelvin and Rossby waves and for the SST mode. Section 5 focuses on dimensional results for the SST mode in the fast-wave limit and distorted physics experiments to test the applicability of this limit in the HGCM are presented in section 6. Because the results of these two sections may be of particular interest to some readers, the sections are structured such that it is possible to skip directly from section 2 to section 5, omitting the detailed analysis of sections 3 and 4.

One of the main conclusions drawn from the behavior of the HGCM in N, and its relationship to behavior found in larger coupled GCMs, is that a range of flow regimes can occur in the coupled system even for relatively small changes in parameters. The experiences of the various coupled GCM efforts show that an understanding of this range of behavior is essential if one hopes to properly understand the phenomena and pitfalls which may occur in attempting to model El Niño in large and expensive models. The results obtained here are used to suggest interpretations of some of the coupled GCM results obtained by other investigators. However, it is worth prefacing this discussion from the outset with the caveat that these results are relevant to a particular subset of flow regimes. The conclusions of this study are not necessarily in contradiction to those of Schopf and Suarez (1987) and Battisti and Hirst (1988) even though the mechanism proposed here for interannual coupled oscillations is different. Possible links between these cases are suggested in section 7.

2. The simple model

The ocean component of the simple model is based on a modified shallow water model with a fixed-depth mixed-layer. This model is intended to be similar to that of Zebiak and Cane (1987) and its implementation by Battisti (1988) in several respects, a choice which is made partly in the hope of understanding the similarities and differences between that model and the hybrid GCM.

The principal, observationally motivated simplification employed in the model derives from the fact that the strongest SST response to upwelling, advection and thermocline depth anomalies is confined to a fairly narrow band along the equator for the phenomena being considered. Both mean and anomalous upwelling act within a degree or two of the equator and the mean thermocline is much shallower in this region. Although meridional advection tends to spread the region of SST anomaly to a somewhat different extent in different regions, the SST anomaly can, for purposes of understanding, be taken to have fixed meridional structure. A useful model may thus be obtained by considering a surface temperature equation for the equatorial band alone. This equation governs the thermodynamics of a box whose depth is that of the surface mixed layer, H_1, roughly 40 m, and whose width, L_y is characteristic of the width of the upwelling (although this proves not to be a very important parameter for this equation in its present application). The longitudinal dependence of this SST anomaly is then multiplied by the assumed meridional structure of the SST anomaly when it is passed into the atmospheric model. This approach is rather different from that of Hirst (1986,1988) in which a simple parameterization of SST dependence on, for

instance, thermocline depth is assumed to apply uniformly in latitude.

The form of the vertical and meridional differencing is important since temperatures outside the box are fixed or parameterized; an upstream advection scheme ensures suitable behavior. Written for total SST, the scheme is

$$\partial_t T + u_1 \partial_x T + \mathscr{H}(w) \frac{w}{H_{1\text{-}1/2}} (T - T_{\text{sub}}) - \mathscr{H}(-v_N) \frac{2v_N}{L_y} (T - T_N) + \epsilon_T (T - T_0) = 0 \quad (1)$$

where T is the temperature of the equatorial surface box and $\mathscr{H}(w) = 1$, if $w > 0$, $= 0$, otherwise, is the Heaviside function. The Newtonian cooling term represents all one-dimensional vertical processes—mixing, sea surface sensible and latent heat fluxes, long and short wave radiation—which tend to move the system toward a radiative–convective–mixing equilibrium in absence of large scale horizontal dynamics in the upper ocean or atmosphere. T_0 represents the SST value at the equator which would occur in this state, say, 29°C, and ϵ_T is the inverse damping time of these combined processes. The surface meridional velocity at the northern boundary of the equatorial box, v_N, is assumed to be equal and opposite the value at the southern boundary, and the off-equatorial temperature a distance L_y north of the equator, T_N, is assumed here to be the same as that south of the equator. The vertical velocity at the bottom of the mixed layer, w, brings up subsurface temperatures, T_{sub}, over a characteristic vertical scale, $H_{1\text{-}1/2}$, which is larger than H_1 but less than the thermocline depth which characterizes shallow water equation dynamics. If one considers a case of easterly imposed winds of large longitudinal scale producing an Ekman-drift meridional circulation with upwelling along the equator and v_N directed poleward, this equation will decay from arbitrary initial conditions toward an equilibrium temperature that is a weighted mean of T_{sub} and T_0,

$$\bar{T} = \left(\frac{w}{H_{1\text{-}1/2}} T_{\text{sub}} + \epsilon_T T_0 \right) \Big/ \left(\frac{w}{H_{1\text{-}1/2}} + \epsilon_T \right), \quad (2)$$

with a decay time $[(w/H_{1\text{-}1/2}) + \epsilon_T]^{-1}$.

For typical climatological values of upwelling, the decay time associated with the dynamics will be on the order of a month over much of the basin, whereas that associated with surface processes will be several times longer. This results in an equatorial cold tongue that is closer to subsurface temperatures than to the radiative equilibrium value. For the case of westerly winds causing downwelling, the vertical advection term does not act but rather the meridional advection term brings in off-equatorial temperatures. Typically T_N will not be that different than T_0 so meridional "inwelling" simply shuts off the cold tongue. The finite differenced continuity equation,

$$2 \frac{v_N}{L_y} = \frac{w}{H_1} - \partial_x u_1, \quad (3)$$

implies that for long zonal scales the temperature decay time scale associated with dynamics will be of the same order of magnitude in both upwelling and downwelling cases.

A parameterization like that of Zebiak and Cane (1987) is adopted for the effect of vertical displacements of the thermocline on the subsurface temperature

$$T_{\text{sub}} = T_s + \gamma h \quad (4)$$

where T_s is the characteristic temperature that would be upwelled from a thermocline undisturbed by dynamics, and h is the departure of the thermocline depth from its no-motion value. A deeper thermocline corresponds to h positive and thus to warmer T_{sub}, with γ on the order of 10^{-1} K m^{-1}. Nonlinear modifications should be included in this equation when considering large thermocline displacements but estimating the correct form of the nonlinearity is not straightforward and the linear relation is sufficient for the present.

This equatorial strip approximation reduces the temperature equation to a partial differential equation in longitude and time only. It makes the interaction with the dynamical equations considerably more tractable since only equatorial values of u_1, w and h are required. Particularly useful simplifications occur for the vertical shear component of the flow when a modified shallow water model with a mixed layer of constant depth is employed, following Cane (1979). The shallow water system governs the dynamics of a constant-density, reduced-gravity layer representing the ocean above the thermocline, while the wind stress is deposited into a shallower, fixed-depth mixed layer and mixed down into the remainder of the shallow water layer by interfacial friction representing turbulent mixing. This differential deposition of wind stress drives a circulation within the shallow water layer which permits the model to reproduce equatorial upwelling and qualitative features of the equatorial surface current/undercurrent dynamics. Denoting the current in the surface mixed layer by u_1 and the specified depth of this layer by H_1, the current in the remainder of the shallow water layer by u_2 and the mean height of this layer by H_2, with $H = H_1 + H_2$, the equations may be written in terms of the vertical mean and vertical difference current,

$$u_m = (H_1 u_1 + H_2 u_2)/H,$$

$$u_d = (u_1 - u_2) \frac{H_2}{H}, \quad (5)$$

defined such that

$$u_1 = u_d + u_m$$

and

$$w = H_1(\partial_x u_d + \partial_y v_d) + H_1(\partial_x u_m + \partial_y v_m)$$
$$\equiv w_d + w_m. \quad (6)$$

Interfacial stress between the ocean layers is assumed proportional to the difference in current between the two layers, $\tau_{\text{interfacial}}/(\rho H_1) = \epsilon_d(u_1 - u_2)$ and time derivatives in the equations for the vertical difference current are neglected relative to this strong damping, yielding purely local equations in space and time (as in Cane and Zebiak 1987). The characteristic meridional length scale of this frictionally driven vertical difference circulation is determined by the damping time scale of vertical mixing: $L_d \equiv \epsilon_d/\beta$. For the purposes at hand, the meridional component of the surface stress, τ^y, may be neglected since wind perturbations are predominantly zonal in the coupled oscillations of interest. With this simplification, the expression for u_d and w_d at the equator are

$$u_d = b_u \frac{\tau_e{}^x}{\rho H} \quad (7)$$

$$w_d = (-b_w + H_1 b_u \partial_x) \frac{\tau_e{}^x}{\rho H} \quad (8)$$

where $b_u \approx H_2/(H_1\epsilon_d)$ and $b_w \approx (H_1/L_d)b_u$ and $\tau_e{}^x$ denotes the equatorial value of the zonal component of the surface stress, τ^x. Henceforth, the variables w_d and u_d will denote the equatorial values of the vertical difference currents, since these values are all that are required in (1). Averaging over a box of width L_y would change the coefficients by factors on the order of unity. The contribution to v_N at the meridional boundaries of the box in the SST equation is, consistent with the continuity equation,

$$v_d = -\frac{L_y}{2H_1} b_w \frac{\tau_e{}^x}{\rho H}. \quad (9)$$

In choosing values for the parameters in this Cane and Zebiak mixed layer, one would like to choose ϵ_d and H_1 such that magnitudes of w_d and u_d and the meridional structure would simultaneously match the ocean GCM. To mimic the meridional extent of the upwelling region and the strength of the upwelling response, a damping $\epsilon_d \sim (2 \text{ days})^{-1}$ is required; to obtain the correct value for u, a value several times smaller would be needed, especially for westerly stress. The advection of momentum which is neglected in these equations can be important and might be better captured by a model such as Schopf and Cane (1982), but for present purposes the linearity and simplicity of the Cane and Zebiak formulation is ideal.

The vertical mean of the momentum equations for the two layers, together with the continuity equation for the shallow water layer are

$$\partial_t u_m - f v_m + g\partial_x h = \frac{1}{\rho H}\tau^x \quad (10)$$

$$\partial_t v_m + f u_m + g\partial_y h = 0 \quad (11)$$

$$\partial_t gh + c_o{}^2(\partial_x u_m + \partial_y v_m) = 0. \quad (12)$$

The stress at the bottom of the shallow water layer has been neglected; damping due to this effect could be included but is weak since vertical mixing drops off sharply below the thermocline. The meridional component of the surface stress has also been dropped as in (7) and (8). The gravity wave phase speed, c_o, is usually chosen to match that of the first or second vertical mode for reasonable thermal structure. Depending upon assumptions regarding the vertical profiles of temperature and momentum deposition, $c_o{}^2/g$ need not be identical to H in (10) when tuning to a vertically continuous model. Loss of heat content by vertical mixing and surface heat transfer is very slow and has been neglected.

The atmospheric model may be written

$$\frac{1}{\rho H}\tau^x = \mathcal{A}(T, y) \quad (13)$$

where $\mathcal{A}$ is a linear but nonlocal function of the T field over the entire basin and of the assumed meridional structure; $\mathcal{A}$ might be, for example, a Matsuno–Gill model (Matsuno 1966; Gill 1980) with heating proportional to SST, a Lindzen-Nigam (1987) model or a linearized version of the Neelin-Held (1987)–Neelin (1988) model, all of which are closely related to a first approximation (Neelin 1989).

The model given by (1), (3), (6)–(13) and a nonlinear version of (4) could be numerically integrated in a basin with the usual boundary conditions in the shallow water equations. It contains essentially the same physics as the Zebiak and Cane (1987) model, albeit stripped down to facilitate derivation of analytic asymptotic results.

3. Scaling arguments

One may now consider scaling arguments for this simple but representative coupled system. For a heuristic derivation in dimensional form of the SST mode results in the fast-wave limit, the reader may proceed directly to section 5. It is conventional to nondimensionalize the shallow water equations on an equatorial β-plane using the equatorial radius of deformation $L_D = (c_o/\beta)^{1/2} \sim 3 \times 10^5$ m as a length scale and $\Delta t_D = (\beta c_o)^{-1/2} \sim 1.5$ days as a time scale where c_o is the oceanic gravity wave speed. For motions of basin scale in the Pacific, this scaling would exaggerate the scale separation between the time scale of oceanic adjustment by equatorial waves and the time scale of temperature change by advection because the radius of deformation in the ocean is an order of magnitude smaller

than the zonal basin scale. To take this into account, a different length scale, L_x, is used for the zonal derivatives and the quantity

$$\delta_L = L_D/L_x \tag{14}$$

is introduced as the ratio between these. For basin scale motions the suitable time scale is

$$\Delta t = \delta_L{}^{-1}\Delta t_D = L_x/c_o, \tag{15}$$

the time scale of wave propagation across the basin. The scale of the meridional velocity is also a factor of δ_L smaller than the conventional scaling, reflecting the small meridional velocities characteristic of equatorial long waves. The conventional scaling is recovered by setting $\delta_L = 1$. The thermocline depth perturbations are scaled in the conventional manner by $c_o{}^2/g$.

As a temperature scale, one can choose $\Delta T = (T_0 - T_s)$, or similar quantity to measure the magnitude of temperature anomalies which can be generated by upwelling, or, in a case where longitudinal temperature gradients in a basic state are more important, $\Delta T = L_x|\partial_x \bar{T}|$. The zonal wind stress from the atmospheric model for a given temperature perturbation field, $\mathcal{A}(T', y)$, is expressed in units of acceleration as it acts on the shallow water layer. When $\mathcal{A}$ is scaled to have an order unity response to an order unity temperature perturbation, the coefficient for the magnitude of the atmospheric response per degree of temperature perturbation will be denoted A. An important scale in the coupled system is thus $A\Delta T$—a measure of the magnitude of the wind stress acceleration on the shallow water layer which can be generated by the feedback of advectively induced temperature perturbations through the atmospheric model.

Nondimensionalizing according to these scales yields:

$$\partial_{t^*} u_m^* - y^* v_m^* + \partial_{x^*} h^* = \frac{\delta_D}{\delta_L}\mathcal{A}^*(T^*, \delta_a y^*) \tag{16}$$

$$\delta_L{}^2 \partial_{t^*} v_m^* + y^* u_m^* + \partial_{y^*} h^* = 0 \tag{17}$$

$$\partial_{t^*} h^* + \partial_{x^*} u_m^* + \partial_{y^*} v_m^* = 0 \tag{18}$$

where starred variables are nondimensionalized and

$$\delta_D = \Delta t_D A \Delta T/c_o \tag{19}$$

is a small nondimensional number measuring the ratio of the conventional equatorial beta-plane adjustment time scale to the time scale of acceleration of currents in the shallow water layer by stress anomalies produced by coupling. In (16) the quantity δ_L, which arose on the lhs, has been divided through to the rhs of the equation where it corrects δ_D for the asymmetry in zonal and meridional scales. In (17) when $\delta_L{}^2$ is small the time derivative of v_m drops out and the equatorial long wave approximation is obtained. In the uncoupled system, this approximation would be the only consequence of the anisotropic scaling, but in presence of coupling the correction to δ_D by δ_L is important. It may also be noted that, even if meridional wind stress anomalies had been retained and assumed to have the same magnitude as the zonal component, they would be multiplied by δ_D rather than δ_D/δ_L, indicating their lesser importance.

The quantity $\delta_a \equiv L_a/L_D$ is the ratio of the atmospheric radius of deformation to the oceanic radius of deformation. It appears in (16) because L_D has been used to nondimensionalize y, while L_a characterizes the meridional length scale of the atmospheric response to temperature anomalies.

Turning to the vertical difference current, $\mathbf{V}_d$, driven by the vertical profile of the deposition of wind stress, the meridional length scale of the Ekman upwelling zone, L_d, is almost the same as the radius of deformation, L_D, so it is not necessary for present purposes to introduce an additional meridional length scale (although caution must be used when taking limits which change L_D). A suitable scale for the nondimensionalization of u_d is $\Delta t_d A \Delta T$ with $\Delta t_d \sim b_u$ being the effective vertical mixing time scale relating the wind stress acceleration to u_d. The same scale applies to v_d, while the vertical component, w_d is further scaled by a factor of H_1/L_D. A useful nondimensional parameter is the ratio of the conventional beta-plane time scale, $\Delta t_D = (L_D/c_o)$, to the time scale of vertical advection by perturbation upwelling

$$\delta_d \equiv (L_D/c_o)\Big/\left(\Delta t_d \frac{H_1}{L_D} A\Delta T \Big/ H_1\right)^{-1}$$
$$= \Delta t_d A \Delta T/c_o. \tag{20}$$

The corresponding ratio for zonal advection by perturbation currents, u_d, is smaller by a factor of δ_L. Notice that, after rearrangement in (20), this parameter, which measures the coupling of vertical difference currents, is analagous to δ_D, which measures the coupling of the vertical mean currents.

A similar nondimensional quantity, δ_c, may be defined for the climatology as the ratio of Δt_D to the time scale of vertical advection by climatological upwelling, $(\bar{W}/H_{1\text{-}1/2})^{-1}$, where $\bar{W}$ is a representative value of $\bar{w}$. Climatological quantities, denoted by overbars, are not divided into $\mathbf{V}_d$ and $\mathbf{V}_m$ components. Scaling the climatological zonal current, $\bar{u}_1$, as $L_x W/H_{1\text{-}1/2}$ (300 cm day^{-1} yields 1.1 m s^{-1}), the corresponding ratio for zonal advection by climatological currents is also δ_c. The climatological advection time scale is also used to nondimensionalize the radiative–convective–mixing damping time scale, ϵ_T, although this is slower than the advection time scale.

For the sake of definiteness in presentation, a linearization of the simple model temperature equation about an upwelling mean state, $\bar{w} > 0$, is considered since this is the most relevant case. Similar scaling ar-

guments would apply more generally. The basic state vertical and horizontal temperature gradients are denoted $\bar{T}_z$ and $\bar{T}_x$. Denoting perturbation quantities by primes, the specific temperature equation under consideration is thus:

$$\partial_{t*}T^{*\prime} + \delta_d u_d^{*\prime}\bar{T}_x^* + \frac{\delta_d}{\delta_L} w_d^{*\prime}\bar{T}_z^* + u_m^{*\prime}\bar{T}_x^* + w_m^{*\prime}\bar{T}_z^* + \frac{\delta_c}{\delta_L}\bar{u}_1^*\partial_{x*}T^{*\prime} + \frac{\delta_c}{\delta_L}\bar{w}^*(T^{*\prime} - H_o^*\gamma^* h^{*\prime}) + \frac{\delta_c}{\delta_L}\epsilon_T^* T^{*\prime} = 0 \quad (21)$$

where $\bar{T}_z$ and γ have been nondimensionalized by $\Delta T/H_1$ and $\bar{T}_x$ by $\Delta T/L_x$; $H_o^* = (c_o^2/g)/H_1$. The time derivative in (21) is scaled exactly as in (16)–(18) by the time scale of zonal adjustment, Δt. As a result, factors of δ_L^{-1} correct several of the terms for the anisotropic scaling, just as on the rhs of (16).

The nondimensionalized vertical difference currents are given by

$$u_d^{*\prime} = b_u^* \mathcal{A}_e^*(T^{*\prime}) \quad (22)$$

$$w_d^{*\prime} = (-b_w^* + \delta_L b_u^* \partial_{x*})\mathcal{A}_e^*(T^{*\prime}) \quad (23)$$

where $\mathcal{A}_e$ is the equatorial value of $\mathcal{A}$. The superscript star will henceforth be dropped from the nondimensional quantities.

For $A\Delta T = 2 \times 10^{-7}$ m s^{-2}, a value which corresponds to stress anomalies of 0.3 dyn cm^{-2} potentially being produced by the atmospheric model for realizable SST anomalies, and an oceanic phase speed of 2.5 m s^{-1}, one obtains $\delta_D = 1.0 \times 10^{-2} \ll 1$. For these same values, $\delta_d = 3.3 \times 10^{-2}$ is almost as small. The largest zonal length scale under consideration is the basin scale over 2π, $L_x = 2.4 \times 10^6$ m, so $\delta_L^{-1} = 8.0$ at largest. Thus both δ_D/δ_L and δ_d/δ_L are fairly small even for coupling of realistic magnitude although the latter approaches order unity at the longest zonal scales. By reducing the magnitude of the atmospheric model response to SST anomalies, or by decreasing the oceanic adjustment time scale by increasing the oceanic wave speed, these parameters can both be made arbitrarily small. A reasonably convincing case can thus be made for considering at least δ_D/δ_L as a small parameter in obtaining asymptotic expressions for the coupled modes. On the other hand,

$$H_o^* \frac{\delta_D}{\delta_L} = (A\Delta T/g)(L_x/H_1) = 0.3$$

will be treated as potentially being of order one, since it is both larger and has a different phase speed dependence than the other terms.

The time scale of advection by climatological currents, $(\bar{W}/H_{1\text{-}1/2})^{-1}$, is one or two months where upwelling is strong. The value of δ_c is thus in the range 0.025 to 0.05 and δ_c/δ_L reaches 0.2 to 0.4 at basin scales. In most cases, this parameter will not be treated as small, especially since one does not usually consider letting the climatology approach zero. It will, however, prove useful to examine a case where all three of δ_c/δ_L, δ_D/δ_L and δ_d/δ_L are taken to be small. Taking the basic state to be fixed, the simplest way to justify this is in the idealized limit where the ocean is assumed to adjust quickly compared to all of the coupled–advective time scales. Specifically, the time scale of oceanic adjustment across the basin must be short compared to all of: 1) the time scale of acceleration of vertical mean currents by the wind stress created by the coupling, as measured by δ_D; 2) the time scale of advection by vertical difference currents due to the coupled wind stress, as measured by δ_d; and 3) the time scale of advection by climatological currents, as measured by δ_c. This limit will be referred to as the "fast-wave limit" since it assumes that the equatorial wave speed, c_o, is sufficiently fast to bring the ocean into dynamic adjustment rapidly compared to changes due to coupling and temperature advection.

The present choice of scaling is not unique. For instance, one might consider re-scaling u'_m, w'_m, and h' by δ_D/δ_L so that the small parameters all occur in the temperature equation. For nonlinear modeling, this would be preferable, but for the linear eigenvalue problem considered here, the results are independent of such changes.

4. Eigenmodes

Consider the eigenvalue problem obtained from the linearized system, (16)–(18) and (21)–(23), assuming a time dependence $\exp(\lambda t)$. Taking all nondimensional variables to be order unity or less, and dropping the superscript $*$, all variables and the eigenvalue are expanded in orders of a small parameter, $\delta = \delta_D/\delta_L$:

$$T' = T^{(0)} + \delta T^{(1)} + \delta^2 T^{(2)} + \cdots$$

$$\lambda = \lambda^{(0)} + \delta\lambda^{(1)} + \delta^2\lambda^{(2)} + \cdots. \quad (24)$$

At zeroth order in δ, the shallow water equations separate from the temperature equation in the sense that one obtains a subset of solutions which correspond exactly to uncoupled modes of the shallow water equations in both frequency and eigenstructure. These modes do also include non-zero temperature components but these are produced diagnostically from the temperature equation once the eigenvalue is known. Coupling (in the sense of modification of the eigenvalue) will occur at next order in δ for these conventional modes.

An additional eigenmode arises in this model whose eigenvalue corresponds to the time derivative in the temperature equation in the limit of small coupling.

This will be referred to as the SST mode, although it may also have large currents and thermocline displacements associated with it. It tends to be more strongly affected by coupling and will be treated separately from the coupled ocean wave modes.

a. Coupled Rossby and Kelvin modes

The scaling arguments above suggest that much information about the behavior of coupled Rossby and Kelvin waves under reasonably realistic conditions can be obtained by examining the case of waves which are weakly coupled in the sense that δ is considered small. In order to obtain simple solutions, a periodic domain in longitude is used rather than a finite basin. Basic state parameters are assumed constant in x and time.

Employing the long-wave approximation [i.e., dropping the $\delta_L{}^2\partial_t v_m$ term in (17)] and writing the shallow water equation component of the model in terms of $q \equiv u + h$ gives

$$\lambda\left(\frac{d^2}{dy^2} + 2 - y^2\right)\tilde{q} + ik\tilde{q} = \delta\left(\frac{d^2}{dy^2} - y\frac{d}{dy} + 1\right)\tilde{A}(y)\tilde{T} \quad (25)$$

where

$$q = \tilde{q}e^{\lambda t + ikx}, \quad \mathcal{A}(T, y) = \tilde{A}(y)\tilde{T}e^{\lambda t + ikx} \quad (26)$$

and the SST equation is given by the Fourier transform of (21).

To obtain asymptotic expressions for the modification of the conventional oceanic modes by coupling, consider $\delta = \delta_D/\delta_L$ to be small in (25). It is unnecessary to assume the SST equation terms to be small in this case, so this limit can always be accessed by turning down the coupling even if δ_c/δ_L and δ_d/δ_L may potentially approach O(1). The results in this "low-coupling limit" thus include the fast-wave limit but do not depend on it, although as the fast-wave limit is approached, they apply for stronger coupling as well. Another limit within the range of validity of these low-coupling limit results will also be introduced, which is roughly the converse of the fast-wave limit in that the time dependence may be neglected in the SST equation for specific modes—this will be referred to as the "Philander limit." Physically, the low-coupling limit depends on having the wave adjustment time scales sufficiently fast compared to the acceleration time scales due to the coupled wind stress that the wave modes maintain their identity to a first approximation. If δ_D/δ_L were not small, the wind stress coupling would strongly modify the oceanic eigenmodes relative to their structure in the uncoupled case.

Expanding (25) in orders of δ yields the usual uncoupled wave modes at zeroth order

$$\tilde{q}^{(0)} = q_n\psi_n, \quad n = 0, 1, 2, \cdots \quad (27)$$

$$\lambda^{(0)} = \frac{ik}{2n-1} \quad (28)$$

where $\psi_n = e^{-y^2}/^2 H_n(y)$, H_n being the Hermite polynomial of order n. The currents and thermocline perturbations associated with each q_n are

$$u_n{}^{(0)}(y) = q_n{}^{(0)}\left(\frac{1}{2}\psi_n - n\psi_{n-2}\right)$$

$$h_n{}^{(0)}(y) = q_n{}^{(0)}\left(\frac{1}{2}\psi_n + n\psi_{n-2}\right)$$

$$v_n{}^{(0)}(y) = ik\frac{2n}{2n-1}q_n{}^{(0)}\psi_{n-1} \quad (29)$$

where only even values of n, corresponding to symmetric modes are of interest here; $n = 0$ corresponds to the Kelvin wave, $n = 2$ to the first Rossby mode, and so on.

The SST equation at zeroth order yields

$$T^{(0)} = -\frac{u_e{}^{(0)}\bar{T}_x + w_e{}^{(0)}\bar{T}_z - \frac{\delta_c}{\delta_L}\bar{w}H_o\gamma h_e{}^{(0)}}{\lambda^{(0)} + \left[\frac{\delta_c}{\delta_L}\bar{w} + \frac{\delta_d}{\delta_L}(-b_w + i\delta_L b_u k)A_e\bar{T}_z + \delta_d b_u A_e\bar{T}_x + \frac{\delta_c}{\delta_L}\bar{u}_1 ik + \frac{\delta_c}{\delta_L}\epsilon_T\right]} \quad (30)$$

where the equatorial value of $\tilde{A}(y)$, denoted A_e, is a complex scalar with $0 < \arg(A_e) < \pi/2$. The complex phase of A_e represents the zonal phase relation between wind stress and SST anomalies. If westerly/easterly anomalies appear in zonal phase with warm/cold water then $\arg(A_e)$ is positive real; if westerly/easterly anomalies appear a quarter wavelength to the west of warm/cold anomalies, then $\arg(A_e)$ is positive imaginary. The magnitude and phase of A_e will depend on k in a manner determined by the particular atmospheric model. The quantities (u_e, w_e, h_e) in (30) denote equatorial values of the shallow water equation variables as these appear in the temperature equation. Specifically, for the first Rossby mode

$$u_e{}^{(0)} = -3q_2{}^{(0)}, \quad h_e{}^{(0)} = q_2{}^{(0)}, \quad w_e{}^{(0)} = -\frac{1}{3}ikq_2{}^{(0)} \quad (31)$$

and for the Kelvin mode

$$u_e{}^{(0)} = h_e{}^{(0)} = \frac{1}{2}q_0{}^{(0)}, \quad w_e{}^{(0)} = iku_e{}^{(0)}. \quad (32)$$

The perturbation to the eigenvalue at next order is obtained by the Rayleigh–Schrödinger technique just as for the steady Schrödinger equation (Nayfeh 1973;

Landau and Lifschitz 1965) with the slight variant that the perturbation "potential" at this order depends on the zeroth order eigenvalue. Proceeding by reduction of order (Bender and Orszag 1978), one puts $\tilde{q}^{(1)}(y) = \tilde{q}^{(0)}(y)\eta(y)$. This yields, after cancellation and multiplication by $\tilde{q}^{(0)}$,

$$\lambda^{(0)} \frac{d}{dy}\left[(\tilde{q}^{(0)})^2 \frac{d}{dy}\eta\right] = \tilde{q}^{(0)}\left(\frac{d^2}{dy^2} - y\frac{d}{dy} + 1\right) \times \tilde{A}(y)\tilde{T}^{(0)} + ik\frac{\lambda^{(1)}}{\lambda^{(0)}}(\tilde{q}^{(0)})^2. \quad (33)$$

Integrating in y with boundary conditions of decay at $\pm\infty$, and integrating the first term on the rhs twice by parts, making use of the properties of ψ_n, gives

$$\lambda^{(1)} = \frac{-\sqrt{2}}{2^n n!(2n-1)} I_n A_e \frac{\tilde{T}^{(0)}}{\tilde{q}_n^{(0)}} \quad (34)$$

where the convention $0! = 1$ is employed and

$$I_n = \frac{(n-1)}{\sqrt{2\pi}} \int_{-\infty}^{\infty} \frac{\tilde{A}(y)}{A_e}(2n\psi_{n-2} - \psi_n)dy. \quad (35)$$

Because of the $e^{-y^2/2}$ dependence of ψ_n, the details of the atmospheric model wind stress outside of an oceanic radius of deformation from the equator will be unimportant for the gravest oceanic modes. Since the atmospheric radius of deformation is much larger than that in the ocean, I_n will be given to zeroth order in δ_a by taking $A(y)$ to be constant in y. For the first Rossby and Kelvin modes, respectively, one has in this approximation

$$I_2 = 2, \quad I_0 = 1 \quad (36)$$

We thus obtain the eigenvalue to first order in δ_D/δ_L for the first Rossby mode

$$\lambda = \frac{ik}{3} + \frac{1}{6\sqrt{2}}\frac{\delta_D}{\delta_L}A_e \times \frac{3i\bar{T}_x - \frac{k}{3}\bar{T}_z + i\frac{\delta_c}{\delta_L}\bar{w}H_o\gamma}{\frac{k}{3} - i\left[\frac{\delta_c}{\delta_L}\bar{w} + \frac{\delta_d}{\delta_L}(-b_w + ik\delta_L b_u)A_e\bar{T}_z + \delta_d A_e b_u \bar{T}_x + \frac{\delta_c}{\delta_L}\bar{u}_1 ik + \frac{\delta_c}{\delta_L}\epsilon_T\right]} \quad (37)$$

and for the Kelvin mode

$$\lambda = -ik + \frac{1}{\sqrt{2}}\frac{\delta_D}{\delta_L}A_e \times \frac{-i\bar{T}_x + k\bar{T}_z + i\frac{\delta_c}{\delta_L}\bar{w}H_o\gamma}{k + i\left[\frac{\delta_c}{\delta_L}\bar{w} + \frac{\delta_d}{\delta_L}(-b_w + ik\delta_L b_u)A_e\bar{T}_z + \delta_d A_e b_u \bar{T}_x + \frac{\delta_c}{\delta_L}\bar{u}_1 ik + \frac{\delta_c}{\delta_L}\epsilon_T\right]}. \quad (38)$$

The correspondence of the terms of (37) and (38) to the SST equation may be seen by referring to (30); in particular, the terms in the denominator refer to T' terms. A large variety of processes affect the stability of these modes and some mechanisms affect others in a non-additive manner. If the terms associated with coupling through w'_d and u'_d are large, the picture becomes complicated, but fortunately, the scaling analysis suggests that their effects are secondary to the extent that δ_d/δ_L is small. Dropping these for simplicity, and redimensionalizing, the dispersion relationships are, for the first Rossby mode

$$\lambda = i\frac{c_o k}{3} + \frac{1}{6\sqrt{2}}A_e \frac{3i\bar{T}_x - \frac{k}{3}H_1\bar{T}_z + i\frac{\bar{w}}{H_{1\text{-}1/2}}\frac{c_o}{g}\gamma}{\frac{c_o k}{3} + \bar{u}_1 k - i\left(\frac{\bar{w}}{H_{1\text{-}1/2}} + \epsilon_T\right)} \quad (37')$$

and for the Kelvin mode

$$\lambda = -ic_o k + \frac{1}{\sqrt{2}}A_e \frac{-i\bar{T}_x + kH_1\bar{T}_z + i\frac{\bar{w}}{H_{1\text{-}1/2}}\frac{c_o}{g}\gamma}{c_o k - \bar{u}_1 k + i\left(\frac{\bar{w}}{H_{1\text{-}1/2}} + \epsilon_T\right)}. \quad (38')$$

The three terms in the numerator in both expressions arise from $u'_m\bar{T}_x$, $w'_m\bar{T}_z$ and $(\bar{w}/H_{1\text{-}1/2})\gamma h'$. For convenience, these contributions to the numerator will be referred to as $N1$, $N2$ and $N3$, respectively, for both modes. Where necessary, the denominator will be referred to as D. The first term in the denominator comes from the frequency of the unperturbed mode; the expressions have been arranged so that this appears as a positive real term. It is expected to be the largest term in the denominator for realistic basic states and dominates as the fast-wave limit is approached, when wave time scales are faster than advective time scales. The second term in the denominator Doppler-shifts this frequency due to temperature advection by the climatological surface current. This can have considerable effect on the Rossby wave, since the westward surface current along the equator is not that much slower than the Rossby wave speed. This current advects the SST perturbations in the direction of propagation of the Rossby mode, thus helping to keep the wave and SST components of the mode in phase for longer and reducing the effective frequency affecting interactions among the coupling terms in (37').

The third term of the denominator, $(\bar{w}/H_{1\text{-}1/2} + \epsilon_T)$, acts as a combined damping term in the SST equation but has a very different effect on the coupled wave modes and can greatly alter the stability properties if it is large. To take an extreme case which exemplifies this, consider the limit of very large $\bar{w}$ in both numer-

ator and denominator. In this case, the SST equation is effectively reduced to $T \approx \gamma h$ which is a case considered by Philander et al. (1984) and also explored by Hirst (1986). The Kelvin wave eigenvalue becomes, for this case

$$\lambda = -ic_o k + \frac{1}{\sqrt{2}} A_e \frac{c_o}{g} \gamma \tag{39}$$

which grows through $\mathrm{Re}(A_e)$, i.e., to the extent that wind stress from the atmospheric model is in zonal phase with the SST perturbation. The Rossby wave is damped for this case. This limit does not hold for reasonable parameter values, but it serves to point out that the $\bar{w}$ term in the denominator can act to favor certain types of instability through its interaction with terms in the numerator. The behavior in this limit contrasts strongly with the behavior when the $c_o k$ term dominates the denominator, as occurs when the fast-wave limit is approached. In the fast-wave limit, for large c_o, the Kelvin wave eigenvalue becomes

$$\lambda = -ic_o k + i \frac{1}{\sqrt{2}} A_e \frac{\bar{w}}{H_{1\text{-}1/2}} \frac{\gamma}{gk} \tag{39'}$$

which is damped by the coupling through $\mathrm{Im}(A_e)$, i.e., to the extent that the zonal phase of the wind stress is in quadrature with the SST perturbation. The Rossby mode is similarly damped. The same term of the denominator, $N3$, measuring the effect of thermocline perturbations, is responsible for both the Kelvin mode growth in the first case and decay in the second, according to how it is influenced by the denominator, and for the Rossby mode decay in both cases.

To provide a terminology for distinguishing between these extremes, a slightly generalized version of the Philander et al. limit of (39) will be considered. The case where the Doppler-shifted frequency in the denominator of (37′) and (38′) can be neglected relative to the other terms of the denominator will be referred to as the *Philander limit.* Physically, this means that for the particular mode in question, the frequency—Doppler-shifted by the advection of SST anomalies—is sufficiently small compared to the damping terms that the $\partial_t T'$ term of the SST equation may be neglected *relative to the other T' terms.* Note that even if a particular mode is reasonably well approximated by the Philander limit, the limit should not be applied to the model as a whole because it will never hold true for the SST mode. Assuming that the effect of the mean surface currents does not actually reverse the sign of the Doppler-shifted frequency, the complex phase of the denominator, $\arg(D)$, will be in the range 0 to $\pi/2$ for the Kelvin wave and $-\pi/2$ to 0 for the Rossby wave. $\arg(D) \approx 0$ occurs as the fast-wave limit is approached and the Philander limit corresponds to the $\pm\pi/2$ case. The Philander limit is thus in some sense the opposite of the fast-wave limit and provides a convenient means of referring to different extremes within the low coupling limit. However, it should be noted that the fast-wave limit is actually approached in two stages for these wave modes. The $c_o k$ term dominates the denominator for smaller c_o than is required for the $N3$ term to dominate the numerator.

The stability properties of the Rossby and Kelvin modes for a case with realistic parameters are summarized in Fig. 1. In addition to standard numerical values used in section 3, the following values have been assumed: $\bar{T}_z = 0.1\ \mathrm{K\ m^{-1}}$, $\bar{T}_x = -0.33 \times 10^{-6}\ \mathrm{K\ m^{-1}}$, $\gamma = 0.1\ \mathrm{K\ m^{-1}}$, $g = 4.2 \times 10^{-2}\ \mathrm{m\ s^{-2}}$, $c_o = 2.5\ \mathrm{m\ s^{-1}}$, $\bar{w}/H_{1\text{-}1/2} = (30\ \mathrm{days})^{-1}$, $\bar{u}_1 = -0.4\ \mathrm{m\ s^{-1}}$, $k = 4.2 \times 10^{-7}\ \mathrm{m^{-1}}$, $\epsilon_T = (125\ \mathrm{days})^{-1}$. These yield values of the complex phase of the denominator, $\arg(D)$, of 21° for the Kelvin wave and −71° for the Rossby wave. If the effect of $\bar{u}_1$ is neglected in the Rossby wave, $\arg(D)$ is reduced to about −49°. In other words the Kelvin wave is reasonably close to the fast-wave limit, as far as the denominator is concerned, while the Rossby wave, because of the effects of Doppler-shifting by the mean currents, is actually not that far from the generalized version of the Philander limit. The complex phase of the atmospheric model, representing the relative zonal phase of wind stress anomalies and SST anomalies, is taken to be 60°. This is reasonable for both the atmospheric model used in the HGCM and the Gill model, although it is possible to get zonal phase shifts in the range from about 45° to approaching 90°, for individual Fourier components, depending on the parameters chosen.

Figure 1 shows the three terms of the numerator for each mode, summed graphically in the complex plane of the numerator. The demi-plane in which the numerator could give instability is shown by shading. It is rotated by an angle $-\arg(A_e) + \arg(D)$ by the effects of the complex phase of the atmospheric model and the denominator. When the sum of the three numerator terms lies in the shaded area, the coupling tends to produce instability; this is determined purely by the model basic state and does not depend on the strength of the coupling at this level of approximation. However, this tendency must be large enough to overcome damping time scales in the ocean model—these have been omitted from (37′) and (38′) for simplicity but would simply appear additively as long as they are small compared to $c_o k$. A coupling strength on the order of $10^{-7}\ \mathrm{m\ s^{-2}\ K^{-1}}$ is required before the coupled instability can overcome a $(200\ \mathrm{day})^{-1}$ damping in the shallow water ocean component of the model.

For the Rossby mode, it may be seen that the $u'_m \bar{T}_x$ term, $N1$, tends to give instability for almost all reasonable values of $\arg(A_e)$ and $\arg(D)$, assuming $\bar{T}_x < 0$, as occurs through most of the Pacific. The $w'_m \bar{T}_z$ term, $N2$, favors instability in the case shown, but would oppose it if $\arg(D)$ were smaller. The $(\bar{w}/H_{1\text{-}1/2}) \times \gamma h'$ term, $N3$, strongly opposes instability due to $N1$ and, in this case, overcomes it so that the net effect of the coupling is to stabilize the Rossby mode. It would

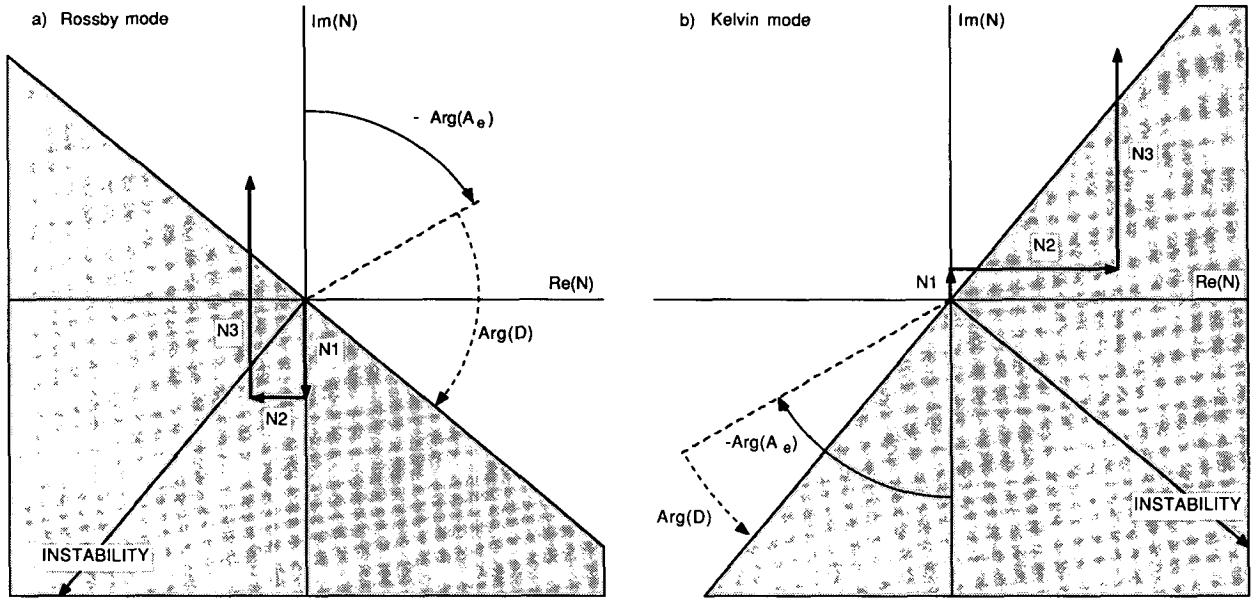

FIG. 1. Effects of various terms on the stability of the coupled Kelvin and Rossby modes according to the dispersion relations (37′) and (38′). The three terms of the numerator, $N = N1 + N2 + N3$, are shown summed in the complex plane. They are associated with the $u'_m\bar{T}_x$, $w'_m\bar{T}_z$, and $(\bar{w}/H_{1\text{-}1/2})\gamma h'$ terms of the SST equation, respectively. The demiplane in which these can produce instability is shaded; it is rotated by the complex arguments of the atmospheric wind stress feedback, $\arg(A_e)$, which represents the zonal phase lag between stress and SST anomalies, and of the denominator, $\arg(D)$, which measures the relative effects of the uncoupled frequency versus damping on the zonal phase of SST anomalies produced by advection. Note $\bar{T}_x < 0$.

(a) Rossby mode: $N1 = 3i\bar{T}_x$, $N2 = -\frac{1}{3}kH_1T_z$, $N3 = i(\bar{w}/H_{1\text{-}1/2})(c_o/g)\gamma$. $D = (c_ok/3) + \bar{u}_1k - i[(\bar{w}/H_{1\text{-}1/2}) + \epsilon_T]$.

(b) Kelvin mode: $N1 = -i\bar{T}_x$, $N2 = kH_1\bar{T}_z$, $N3 = i(\bar{w}/H_{1\text{-}1/2})(c_o/g)\gamma$. $D = c_ok - \bar{u}_1k + i[(\bar{w}/H_{1\text{-}1/2}) + \epsilon T]$.

not be difficult to find unstable basic states, however. A reduction in γ or an increase in $\bar{T}_x$ would accomplish this by reducing $N3$ or increasing $N1$. Either of these would be aided by an increase in $\arg(A_e)$ (i.e. westerlies farther to the west of warm SST). Such destabilization could also be accomplished by decreasing $\bar{w}$, although in this case two opposing effects must be taken into account. Both the $N3$ term and $\arg(D)$ depend upon $\bar{w}$. While the former strongly opposes instability, the closeness of this mode to the Philander limit, with large $\arg(D)$, acts to favor instability. Since decreasing $\bar{w}$ decreases both of these terms, the net effect on stability is small, although a sufficient reduction could produce a weak tendency to instability for the case shown.

For the Kelvin mode, the $u'_m\bar{T}_x$ term, $N1$ tends to weakly oppose instability. The $(\bar{w}/H_{1\text{-}1/2})\gamma h'$ term, $N3$, acts strongly to oppose instability, as in the Rossby wave. The $w'_m\bar{T}_z$ term, $N2$, on the other hand, is much more significant than in the Rossby case and tends to produce instability. The net result is slightly stable for the case shown. Here $\arg(A_e)$ tends to oppose instability for this mode; instability is favored when the zonal phase lag between stress and SST anomalies is reduced; $\arg(D)$ again aids instability, although its effects are small in this case, i.e. the Kelvin wave is closer to the fast-wave limit than to the Philander limit. However, as noted in (39), if $\bar{w}$ were greatly increased, the effects of increasing $\arg(D)$ would cause all terms of the numerator to become destabilizing, especially $N3$ which under normal circumstances has the opposite effect. In other words, all coupled terms tend to destabilize the Kelvin wave in the Philander limit.

The physical mechanism responsible for destabilizing the Kelvin wave is vertical advection of the mean vertical temperature gradient by upwelling anomalies produced by zonal convergence of u'_m. Because the frequency of the mode is approximately determined by the properties of the uncoupled mode, these upwelling anomalies determine the SST anomaly itself, rather than the SST tendency. The SST anomalies will tend to appear in zonal quadrature with the upwelling anomaly since the uncoupled mode is purely propagating—the advection anomalies may be thought of as moving at a fixed phase speed, leaving temperature anomalies in their wake. To the extent that the wind stress is in zonal phase with the SST anomaly, the currents produced by this stress will feed back positively on the upwelling anomaly, producing growth. For the Rossby mode, the destabilizing tendency is due to zonal advection of the (negative) mean zonal temperature gradient by the perturbation zonal velocity. The SST anomalies are determined by a slightly more complicated balance in this case, since the SST damping term is significant and must be taken into account along with the frequency of the uncoupled mode. In the Philander limit, when the frequency is negligible compared

to the damping, the SST anomalies have opposite zonal phase to the advection anomaly to maintain balance in the SST equation; in the fast-wave limit when the frequency dominates, the SST anomalies appear in quadrature, although in the opposite direction to the Kelvin wave case, since the phase speed is negative. The realistic case has SST anomalies with intermediate zonal phase given by arg(D). Physically, arg(D) represents the difference in zonal phase of the SST anomalies in presence of both propagation and damping relative to the zonal phase due to propagation alone. When the combined zonal phase shift due to this effect and the zonal phase of the atmospheric model is 90°, the wind stress is optimally positioned to feed back positively on to the currents to give growth by $u'_m\bar{T}_x$.

It may also be seen from Fig. 1 that for most of the realistic cases, whether stable or unstable, the effect of coupling is to slow the mode relative to its uncoupled phase speed. All three terms in the Kelvin wave in Fig. 1b act to produce a positive imaginary correction to the frequency, which opposes the zeroth order eastward propagation. For the Rossby wave case shown, the net effect of the numerator terms is to produce a negative imaginary, i.e. eastward, correction to the phase speed, thus slowing the zeroth order propagation. However, it is possible to find cases where the reverse occurs—the destabilizing $N1$ term in the Rossby wave actually tends to increase the phase speed of the mode due to the effects of the denominator.

The analytic results given by (37′) and (38′) may be compared with the numerical results of Hirst (1986, 1988) who used a shallow water model without a surface layer, with an SST equation which contains advection by the shallow water currents (u_m in the present notation) and a parameterized tendency for SST to increase as the thermocline deepens, applied at all latitudes. The latter mechanism corresponds approximately to the $(\bar{w}/H_{1\text{-}1/2})\gamma h'$ term of the SST equation in the present model. Hirst found that the zonal advection mechanism tends to cause decay of the Kelvin wave and to destabilize the Rossby wave, while the Kelvin wave is unstable only in a limit corresponding to (39). Although his model does not include the apparently important $w'_m\bar{T}_z$ term or the $\bar{u}_1$ and $\bar{w}/H_{1\text{-}1/2}$ terms, the analytic results are consistent with his when these terms are dropped, and the numerical results suggest that the asymptotic expressions hold over a very considerable range of coupling.

The complexity of the parameter dependence evident in Fig. 1 makes the analytic results particularly useful, for instance, in deducing the differing roles of the mean upwelling in both favoring and opposing instability and the dependence of this effect on other parameters. They prove similarly helpful in explaining the secondary instability found in the HGCM results. The second mode of variability, which arises above the secondary bifurcation in the HGCM, has small meridional velocities and is symmetric about the equator with maximum zonal velocity and heat content anomalies on the equator and confined near it. Its phase speed, about 1.5 to 2 m s^{-1} is only a little less than that of an equatorial Kelvin wave. A natural explanation is the growth and equilibration of unstable coupled Kelvin waves, although there was previously no known mechanism which could produce these for realistic parameters, nor account for their growth during the warm phase of the ENSO oscillation. At the same time, it is of interest to understand why no mode is seen in the HGCM experiments which looks like a coupled Rossby wave.

Although the secondary bifurcation in the HGCM occurs on a periodic solution, the ENSO-period oscillation is sufficiently slow that it may be regarded as approximately stationary compared to the Kelvin wave period. Under this two-timing assumption, it suffices to consider basic state values characterizing warm and cold phases of the interannual oscillation, respectively, in the Kelvin wave dispersion relation (38′). It may be seen that for the reasonably large values of $\bar{w}$ used in Fig. 1, the $N3$ term stabilizes both the Kelvin and Rossby modes. During the cold phases of the interannual oscillation, increased upwelling further stabilizes both modes. During the warm phases, the upwelling is greatly reduced across much of the basin resulting in a great reduction in the $N3$ term. In the Rossby mode, arg(D) is also greatly reduced when the upwelling is small, so the mode remains stable on the whole. In the Kelvin wave, the effects of arg(D) are not nearly as important so the reduction of $N3$ permits the mode to become unstable due to the effects of $N2$. The Kelvin wave instability thus arises from the $w'_m\bar{T}_z$ term of the SST equation and is modulated by the effects of the $(\bar{w}/H_{1\text{-}1/2})\gamma h'$ term which tends to shut it off during the cold phase. In the HGCM, this effect is enhanced because the effective arg(A_e) is smaller during the warm phase than under normal conditions when the nonlinearity tends to shift the atmospheric model response to SST anomalies westward toward the region of warmest water.

These results also suggest that it is not surprising to find no Rossby wave instability in a system which tends to give Kelvin wave instability, and vice versa, since important mechanisms tending to destabilize the one usually tend to stabilize the other. A potentially important exception to this occurs in the case of more modest upwelling or smaller effect of subsurface temperatures, i.e. a smaller $(\bar{w}/H_{1\text{-}1/2})\gamma h'$ term. Then both Rossby and Kelvin modes can simultaneously become unstable as the Philander limit is approached by reducing the phase speed c_o. Overall, because of the competition between opposing terms in the growth rate, both coupled Kelvin and Rossby wave instability appear to be quite sensitive to parameter changes. Models with different basic states and parameterizations may thus be expected to give differing results. The SST mode, on the other hand, may be expected to prove

more robust since all the coupling mechanisms contribute to growth, including the $(\bar{w}/H_{1\text{-}1/2})\gamma h'$ mechanism which tends to stabilize the Kelvin and Rossby modes.

b. The SST mode

When $\delta = \delta_D/\delta_L \ll 1$, the remaining eigenmode of the system, the SST mode, has zero u'_m, w'_m and h' components at zeroth order. These variables appear at first order since they are of the same order as the wind stress term. However, the effects of these first order variables on the SST equation cannot necessarily be neglected. The SST mode thus tends to be more strongly affected by coupling than the ocean wave modes and further assumptions are required to obtain simple solutions. For instance, if the $(\bar{w}/H_{1\text{-}1/2})\gamma h'$ term is less significant than estimated from the scaling, i.e. if

$$\frac{\delta_c}{\delta_L} H_o^* \frac{\delta_D}{\delta_L} \ll 1$$

but at least one of δ_d/δ_L, δ_c/δ_L or δ_d are of O(1), then the SST mode separates completely from the shallow water system at zeroth order, yielding

$$\lambda^{(0)} = -\frac{\delta_c}{\delta_L}(\bar{w} + \epsilon_T + ik\bar{u}_1) + \frac{\delta_d}{\delta_L} b_w A_e \bar{T}_z - \delta_d b_u A_e \bar{T}_x$$

$$\tilde{w}_d{}^{(0)} = -b_w A_e \tilde{T}^{(0)}$$

$$\tilde{u}_d{}^{(0)} = b_u A_e \tilde{T}^{(0)} \qquad (40)$$

and $u_m{}^{(0)} = w_m{}^{(0)} = h_m{}^{(0)} = 0$. At next order a series solution may be obtained for the correction to the eigenvalue, currents and thermocline displacement. The terms $\bar{w}$ and ϵ_T tend to give damping in (40) which is opposed by the $w'_d\bar{T}_z$ and $u'_d\bar{T}_x$ growth terms. When the coupling approaches zero, this mode is one of pure temperature decay.

However, the scaling analysis suggests that the effects of subsurface temperature anomalies on the SST equation are rather important, i.e., one should treat

$$\frac{\delta_c}{\delta_L} H_o^* \frac{\delta_D}{\delta_L} \sim O(1).$$

When this is true, the SST mode then becomes linked to the shallow water component of the model through the $(\bar{w}/H_{1\text{-}1/2})\gamma h'$ term. In general, the SST mode can be affected by the effects of wave propagation in the shallow water equations through this linkage, despite the low-coupling assumption of small δ_D/δ_L. While this case is potentially of considerable interest to the coupled problem, it appears difficult to treat analytically. However, a very simple solution may be obtained which includes the linkage of the SST mode to the shallow water equations through $(\bar{w}/H_{1\text{-}1/2})\gamma h'$, in the case where all of δ_D/δ_L, δ_d/δ_L and δ_c/δ_L are small and can be treated as $O(\delta)$. Since these terms measure the relative time scales of various coupling effects compared to the time scale of wave propagation across the basin, this always holds true as the fast-wave limit is approached, when the time scales of wave propagation across the basin are small.

In this fast-wave limit case, not only does the SST equation separate from the shallow water equation at zeroth order, implying that $\mathbf{V}_m{}^{(0)} = 0$, but the eigenvalue corresponding to the SST mode is also zero at this order. The eigenvalue is of order δ and is obtained from the $O(\delta)$ SST equation, while the $O(\delta)$ shallow water equations are simply

$$-yv_m{}^{(1)} + \partial_x h^{(1)} = \mathcal{A}(T^{(0)}) \qquad (41)$$

$$yu_m{}^{(1)} + \partial_y h^{(1)} = 0 \qquad (42)$$

$$\partial_x u_m{}^{(1)} + \partial_y v_m{}^{(1)} = 0. \qquad (43)$$

The solution for (41)–(43) is familiar; the currents are in Sverdrup balance (Sverdrup 1947) and

$$\partial_x h^{(1)} = (1 - y\partial_y)\mathcal{A}(T^{(0)}, \delta_a y). \qquad (44)$$

The equatorial value of $h^{(1)}$, is independent of the meridional structure of the wind stress:

$$\partial_x h_e{}^{(1)} = \mathcal{A}_e(T^{(0)}). \qquad (45)$$

The wind stress is balanced by the pressure gradient along the equator in this mode since the ocean has come into adjustment rapidly compared to the slow time scale.

The contribution of the vertical mean currents to the vertical velocity, w_m, is identically zero at this order. When the atmospheric wind stress varies slowly in y compared to the oceanic radius of deformation, the horizontal currents $u_m{}^{(1)}$ and $v_m{}^{(1)}$ also become small. Since

$$\partial_x u_m{}^{(1)} = \partial_y{}^2 \mathcal{A}(T^{(0)}, \delta_a y), \qquad (46)$$

advection by u_m belongs to the higher order effects and may be neglected in the order δ temperature equation when $\delta_a{}^2 \ll 1$.

This limit of the SST mode is thus characterized by a balance between wind stress and pressure gradients with very small vertical mean currents (order $\delta_a{}^2\delta$), while the temperature and vertical difference currents are large (order unity). Because the mode in this case has a slow (order δ) time scale of evolution, it may appropriately be referred to as the slow SST mode in the fast-wave limit. The propagation characteristics are determined entirely by the evolution of the temperature equation, coupled nonlocally through the wind stress to the frictionally driven vertical difference currents, and to the temporally-adjusted thermocline perturbations.

The assumption that δ_c/δ_L and δ_d/δ_L are small—i.e. that the equatorial wave speed, c_o, is sufficiently fast

compared to the advection–coupling time scales that the ocean comes into dynamic adjustment *even in the zonal direction* much more quickly than the SST mode evolves due to coupling and temperature advection—is not strictly valid for motions of basin scale in the Pacific. However, the resulting equations are sufficiently handy that it is worth employing this expansion as a convenient fiction. This limit of the SST mode appears to be the simplest available solution which may be considered as a possible analog of the interannual oscillation found in some coupled models, such as the HGCM.

If none of the parameters are assumed small, analytic solutions become increasingly cumbersome, involving series expansions of the atmospheric model y-dependence. The SST mode becomes coupled to the long Rossby and Kelvin oceanic wave modes and the time scale of wave propagation may potentially become important in the SST mode eigenvalue. When δ_D/δ_L is taken to be O(1), the wave modes also begin to lose their identity due to coupling. However, the scaling suggests that the SST mode for realistic parameters may be expected to share qualitative characteristics with the slow SST mode in the fast-wave limit, for which there is a simple, analytic expression. Thus, it is to the fast-wave limit that we turn for a qualitative understanding of the processes giving rise to the instability of the SST mode.

5. The slow SST mode in the fast-wave limit

The dimensional equations for the SST mode in the fast-wave limit may be obtained from the scaled equations of the previous sections, retaining terms to order δ. However, it is worthwhile to restate the derivation heuristically in dimensional form. The feedback of temperature anomalies producing wind stress anomalies and thus oceanic anomalies, which in turn give temperature *tendencies* through anomalous advection, defines characteristic coupling time scales. If these time scales are much slower than the time scale of wave propagation across the basin, then the eigenvalue problem separates into two classes of modes: the slow SST mode and the (relatively fast) modified oceanic modes. Within the SST mode, the ocean dynamics tends to come into balance quickly on the interannual time scales over which SST is evolving. In the idealized limit in which ocean wave modes are made very fast, the SST mode remains slow and its currents and equatorial height field are in Sverdrup balance with the wind stress. Although this is presented here as an idealization, McPhadden and Taft (1988) show evidence that this equatorial balance, (50), holds to a good approximation on annual and longer time scales in observations. The relevance of the fast-wave limit to practical situations is greatly aided by the fact that higher meridional ocean wave modes, which have slower time scales, contribute relatively little to the adjustment of the near-equatorial fields, and thus to the coupling, compared to the faster gravest meridional modes.

For the SST equation linearized about a basic state with mean upwelling, and assuming a time dependence $\exp(\lambda t)$, the equations for the SST mode in the fast-wave limit are

$$\lambda T' + w'_d \bar{T}_z + \frac{\bar{w}}{H_{1\text{-}1/2}}(T' - \gamma h'_e) + u'_d \bar{T}_x + \bar{u}_1 \partial_x T' + u'_m \bar{T}_x + \epsilon_T T' = 0 \quad (47)$$

$$w'_d = (-b_w + H_1 b_u \partial_x)\mathcal{A}_e(T') \quad (48)$$

$$u'_d = b_u \mathcal{A}_e(T') \quad (49)$$

$$g\partial_x h'_e = \mathcal{A}_e(T') \quad (50)$$

$$\partial_x u'_m = \beta^{-1}\partial_y{}^2 \mathcal{A}(T', y). \quad (51)$$

The off-equatorial values of h' and v'_m may be obtained diagnostically from (44) and Sverdrup balance respectively and $w'_m = 0$. The u'_m term is small and will be dropped from the temperature equation in subsequent discussion, employing the approximation that the atmospheric wind stress varies slowly in y compared to the oceanic radius of deformation. The smallness of u_m also suggests that the above equations may be applied in a basin of finite zonal extent with oceanic boundary conditions automatically satisfied to a good approximation (although a boundary condition for (50) is still required). The primary difference between the zonally periodic case and the finite-basin case is thus the extent of the SST anomalies affecting the atmospheric model (excluding zonally symmetric modes from consideration). Examination of the zonally periodic case may be justified as an approximation to the case where the influence of the nonoceanic part of the domain on the atmospheric response does not penetrate significantly into the ocean domain, and where zonal inhomogenieties of the ocean basic state are do not strongly restrict the effects of coupling within the ocean basin.

With this justification, the response may again be examined for SST anomalies of the form $T' = \tilde{T}\exp(ikx)$. The equatorial atmospheric model response $\tilde{\mathcal{A}}_e(T') = A_e\tilde{T}$, is all that is required, where A_e is a complex scalar, its phase representing the amount by which the zonal phase of the wind stress at the equator differs from that of the temperature for the wavenumber k Fourier component. Since westerly wind stress occurs over and to the west of a warm anomaly, $\mathrm{Re}(A_e) > 0$ and $\mathrm{Im}(A_e) > 0$. For the particular case of a Gill (1980) model with heating proportional to SST and expanding the assumed y-structure of the SST anomalies as

$$S(y) = \sum_{n=0}^{\infty} S_n \psi_n(y/L_a),$$

where L_a is the atmospheric radius of deformation,

$$A_e = -A \sum_{n=0}^{\infty} (-1)^{n/2} \frac{n!}{\left(\frac{n}{2}\right)!} \frac{2n-1}{2(n-1)} \times \left[(n-1)S_n + \frac{1}{2} S_{n-2}\right] \frac{(2n-1)\epsilon_a{}^2 + ik\epsilon_a}{(2n-1)^2\epsilon_a{}^2 + k^2} \quad (52)$$

where ϵ_a is the atmospheric damping expressed as an inverse length scale, A is the proportionality constant for the amplitude of the atmospheric response and the sum is taken only over even values of n with $S_{-2} \equiv 0$. Both real and imaginary parts of A_e depend on the zonal wavenumber. For reasonable values of ϵ_a, and scales less than or on the order of the Pacific,[1] the atmospheric response, especially $\mathrm{Re}(A_e)$ tends to be larger at larger zonal scales. The emphasis on the equatorial value of the zonal wind stress from the atmospheric model, A_e, in these results is in accord with the findings of Harrison (1989), upon forcing an ocean GCM with full versus near-equatorial observed wind stress anomalies, and with experiments on near-equatorial versus full winds by Battisti (1988) in a coupled model.

For the case of a periodic basin, with $\bar{w}$ and other basic state parameters independent of longitude, the dispersion relation for the slow SST mode in the fast-wave limit is simply

$$\lambda = \underbrace{A_e b_w \bar{T}_z}_{\text{(A1)}} - \underbrace{A_e H_1 b_u ik \bar{T}_z}_{\text{(A2)}} + \underbrace{\frac{1}{ikg} A_e \gamma \frac{\bar{w}}{H_{1\text{-}1/2}}}_{\text{(B)}} - \underbrace{A_e b_u \bar{T}_x}_{\text{(C)}} - \underbrace{\left(\frac{\bar{w}}{H_{1\text{-}1/2}} + \epsilon_T\right)}_{\text{(D)}} - \underbrace{ik\bar{u}_1}_{\text{(E)}}. \quad (53)$$

The correspondence between the terms of (53) and the terms of the linearized SST equation, (47), is given in Table 1, which also summarizes the contribution of each term to the propagation and growth characteristics of the SST mode. The first four terms all contribute to instability of the mode. The terms A1 and A2 are associated with anomalous upwelling of mean temperature gradients. The main effect is that of A1 which is due to the upwelling perturbations associated with circulation in the vertical–meridional plane, while A2 is due to upwelling associated with zonal divergence. The latter is small except at small zonal scales. Although the meridional temperature gradient does not appear explicitly in A1, it may be taken to represent the combined effects of meridional as well as vertical advection by vertical–meridional circulation anomalies. This is demonstrated in the Appendix by consideration of a slightly more complex finite differencing scheme.

Term B is due to the effect of thermocline perturbations on the subsurface temperature, which is communicated to the surface temperature equation by the mean upwelling. The effect of term B is similar to the instability mechanism due to an assumed dependence of SST on thermocline depth considered by Philander et al. (1984) and Hirst (1986). Term C is due to advection of mean zonal temperature gradients by anomalous currents. This term is different than the zonal advection mechanism considered by Hirst (1986) since the advection is due to vertical difference currents introduced by inclusion of a mixed layer. Here, the destabilizing effect appears in the SST mode. The term D is a damping term which tends to oppose instability. It includes not only the damping time scale due to vertical mixing and surface fluxes, ϵ_T, but also the dynamical damping time scale, $\bar{w}/H_{1\text{-}1/2}$, which is of primary importance. The term E is just advection of the temperature perturbation by the mean current which can affect the propagation of temperature anomalies but not the growth. Dependence of the terms of (53) on zonal length scale enters both through the explicit dependence on k and through A_e, as may be seen from (52). Long zonal scales tend to be more favorable to growth.

Terms C and A2 contribute to growth through the imaginary part of the atmospheric model coefficient, $\mathrm{Im}(A_e)$, and tend to give eastward propagation due to $\mathrm{Re}(A_e)$. Terms A1 and C contribute to growth due to $\mathrm{Re}(A_e)$ and tend to give westward propagation due to $\mathrm{Im}(A_e)$. In other words, to the extent that the atmospheric model zonal wind stress is in phase with the SST anomaly along the equator, the coupled mode will tend to grow through A1 and C and propagate eastward due to A2 and B. To the extent that westerly anomalies appear in quadrature (90° to the west) of a warm anomaly, the coupled mode will grow through B and A2 and propagate westward due to A1 and C.

The basic state coefficients in coupled GCMs are far from being zonally uniform, so the simple periodic-basin dispersion relation (53) can give only qualitative insight into the relative contributions of the various mechanisms, especially in the case of zonal advection, since the region of large $\bar{T}_x$ is actually quite restricted. It may be seen from (53) that a diagnostic analysis of the surface temperature equation of the ocean component would not by itself give much insight into the relative importance of these processes to the coupled instability. The coefficients of coupling by the atmospheric model back to the dynamics of the mixed layer and thermocline must also be known to estimate the

[1] The limits $k \to 0$ and $\epsilon_a \gg k$ should both be avoided in considering the Gill model. This is because a major deficiency of this model is its poor simulation of the zonally symmetric part of the flow in the vicinity of the equator, as pointed out by Neelin (1988) on practical grounds and Lindzen and Nigam (1987) on theoretical grounds. Similar problems arise when ϵ_a is large compared to k.

TABLE 1. Terms of the dispersion relation (53) for the SST mode in the fast-wave limit summarized by correspondence to terms of the linearized SST equation, (47), and their contribution to propagation and growth characteristics of the mode. The real and imaginary parts of the atmospheric equatorial response $\mathrm{Re}(A_e)$ and $\mathrm{Im}(A_e)$ indicate the extent to which the Fourier component of the zonal wind stress is in phase or in quadrature, respectively, with temperature in the zonal direction.

	Term of SST mode dispersion relation					
	$A_e b_w \bar{T}_z$	$-A_e H_1 b_u ik\bar{T}_z$	$\frac{1}{ikg} A_e \gamma \frac{\bar{w}}{H_{1-1/2}}$	$-A_e b_u \bar{T}_x$	$-\left(\frac{\bar{w}}{H_{1-1/2}} + \epsilon_T\right)$	$-ik\bar{u}_1$
Referred to in text as	(A1)	(A2)	(B)	(C)	(D)	(E)
From term in SST equation	$w'_d \bar{T}_z$	$w'_d \bar{T}_z$	$-\frac{\bar{w}}{H_{1-1/2}} \gamma h'_e$	$u'_d \bar{T}_x$	$\frac{\bar{w}}{H_{1-1/2}} T' + \epsilon_T T'$	$\bar{u}_1 \partial_x T'$
Propagation tendency	West	East	East	West	—	(as $\bar{u}_1$)
Growth by	$\mathrm{Re}(A_e)$	$\mathrm{Im}(A_e)$	$\mathrm{Im}(A_e)$	$\mathrm{Re}(A_e)$	(Damping)	—

contribution of each term and the form of this feedback is different for the different mechanisms. An exception is the comparison of terms A1 and C—because these have the same form, comparison of the corresponding SST equation terms does give information about their relative importance. Insofar as the basin mode of the HGCM resembles the periodic-domain mode of (53), and using values of basic state parameters characteristic of averages across the basin, for a mode with a zonal scale characteristic of the Pacific one finds that the contribution of A2 is small but the other three growth terms are of the same order of magnitude. The growth rate is a balance between the damping term D, and the sum of terms A1, B and C, with C less important than the other two. The damping and growth terms both have time scales on the order of a month to a few months; where these cancel exactly the bifurcation occurs.

In the HGCM experiments of N, three different effects were considered which moved the system toward or away from the bifurcation. Increasing the heat content of the oceanic basic state was found to move the system away from instability due to associated changes in the vertical temperature profile. The loss of instability is caused by a reduction in $\bar{T}_z$ in term A1 and a reduction in γ in term B. Another parameter used to change the stability properties of the system was a relative coupling coefficient which reduced the atmospheric wind stress anomalies relative to a run with sustained oscillations. The effect of this coefficient in (53) is simply to reduce the atmospheric feedback parameter, A_e, proportionately and thus to reduce all of the instability terms. The other effect which moved the system across the bifurcation was a reduction of the mean wind stress in the climatology, resulting in a new basic state which was unstable to the slow coupled mode. The reduction of the climatological wind stress had several effects on the basic state: a substantial decrease in $\bar{w}$ and $\bar{T}_x$, with $\bar{T}_z$ and γ tending to decrease in the east and increase in the west of the basin. If one considers the effect of these changes on the instability terms, they appear on the whole to be stabilizing. In particular, terms B and C are substantially reduced by the decreases in $\bar{w}$ and $\bar{T}_x$. The reason that the basic state goes unstable is that the damping term D is substantially reduced by the reduction in $\bar{w}$, while the instability term A1 remains relatively unchanged.

The contributions to the propagation speed of terms A1, B and C of (53) are of similar magnitude but opposing sign. The mode tends to propagate westward due to the substantial zonal phase lag between wind stress and SST (e.g., westerly wind anomalies occur to the west of a warm anomaly) which permits the combined effects of A1 and C to outweigh the eastward tendency of B. In the periodic-basin mode represented by (53), the frequency of the oscillation is determined by the phase speed of the mode, with cold phases following in the wake of each warm phase due to the easterlies to the east of the warm anomaly and vice versa. The period of the SST mode in this fast-wave limit, periodic-basin case would be sensitive to the phase of the wind stress relative to the SST anomaly in the atmospheric model, and to the relative importance of the anomalous upwelling and thermocline depth instability mechanisms. However, this sensitivity would be moderated in the full model by the fact that the fast-wave limit does not apply if the slowness assumption is violated. If the period suggested by (53) were much shorter than a year, the time scale of wave propagation across the basin could not be assumed small compared to the coupled time scale and the fast-wave limit would break down.

Another feature worth examining in the slow SST mode is the form of thermocline perturbation anomalies which are in balance with the wind stress according to (44). As an example, consider the case of a wind stress with a Gaussian meridional structure with a half-width given by the atmospheric radius of deformation, L_a. The y-structure of the thermocline depth is then given by

$$gikh = A_e\tilde{T}\exp[-y^2/(2L_a^2)](1 + y^2/L_a^2) \quad (54)$$

with maxima occurring at one atmospheric radius of deformation off the equator. This form suggests that caution should be exercised when attempting to identify heat content anomalies in observations with oceanic Rossby waves. The slow SST mode can have qualitatively similar features even though it is completely independent of the characteristics of Rossby wave propagation in the fast-wave limit.

The question of locality versus nonlocality may also be considered for the SST mode in the fast-wave limit. Although the atmospheric component of the model is always nonlocal to an extent determined by the atmospheric model damping radius, the growth terms A1, A2 and C are essentially local, as far as the ocean component is concerned, since they are due to advection by anomalous currents produced by local wind stress. The thermocline perturbation term, B, is nonlocal; although the thermocline *gradient* is in local balance with the wind stress according to (50), the thermocline perturbation which enters the growth term effectively depends on a zonal integral of wind stress. The comparable importance of local and nonlocal effects within the ocean component is in accord with GCM experiments by Harrison (1989) who examined SST anomalies produced by observed wind stress anomalies for the 1982–83 event compared to SST anomalies produced when the wind stress anomalies were restricted to subregions of the basin. Locally forced anomalies in the eastern Pacific were found to be roughly twice as large as those forced remotely by winds in the western Pacific. Nonlocal effects in the SST mode are, of course, communicated by oceanic wave modes, but in the fast-wave limit this communication is assumed to occur quickly compared to the evolution of the mode.

Finally, it should be noted that the fast-wave limit cannot be examined in a coupled model such as the HGCM by reducing the coupling of the anomalies because the damping of SST by the mean upwelling would not be reduced proportionately. As a result, the mode would decay rapidly. This is the reason for distinguishing between the fast-wave limit and the low-coupling limit, as discussed in section 4.

6. Distorted-physics experiments

Motivated by the scaling analysis of the section 3, one can attempt to design experiments with the hybrid GCM coupled system in order to test the extent to which the fast-wave limit of the SST mode is relevant to the oscillation observed in the HGCM. Because the SST mode can also be affected by wave propagation time scales for the most realistic scaling, the hypothesis to be tested needs to be phrased more precisely. The Schopf and Suarez (1988) delayed oscillator hypothesis and the fast-wave limit may be taken as the two extreme paradigms of behavior for interannual oscillations. In the case of the delayed oscillator, if the delay due to information propagation across the basin is too small, the unstable mode does not oscillate at all but undergoes pure exponential growth. In the fast-wave limit, even if the wave speed is very fast—that is, so fast that the ocean may be regarded as coming instantaneously into adjustment on the time scale of the slow mode—there is still a low frequency period due to propagation of the slow SST mode. The question to be examined may be posed as follows: is the (uncoupled) equatorial wave propagation time scale across the basin essential to the existence of the oscillation? Subsidiary questions would be: are the time scale and nature of the oscillation much the same in the fast-wave limit as they are with realistic parameter settings?

These questions can be answered in a straightforward manner in any numerical coupled model by means of *distorted physics experiments* in which the wave speed of the model is artificially changed without altering the steady balance in any of the model equations. This trick has been used, for instance, by Bryan and Lewis (1979), to accelerate the spinup of an ocean model to equilibrium. In their computational application, wave speed is reduced to relax numerical stability criteria and reduce the cost of integration to equilibrium. In the present application, motivated by hypothesis testing, we rather perversely wish to do the opposite, which has the side effect of increasing computational costs.

Slightly different variants of the technique are proposed for shallow water models and primitive equation models. In the primitive equation case, the time derivatives of the momentum equations are multiplied by an artificial factor, δ_{art}, relative to the time derivatives in the temperature equations. For comparison, we illustrate the primitive equation version in the shallow water equations. The modification would appear as

$$\delta_{\text{art}}\partial_t u - fv + g\partial_x h = \mathcal{A} \quad (55a)$$

$$\delta_{\text{art}}\partial_t v + fu + g\partial_x h = 0 \quad (55b)$$

$$\partial_t gh + c_o^2(\partial_x u + \partial_y v) = 0 \quad (55c)$$

The equatorial Kelvin wave speed becomes $c_o\delta_{\text{art}}^{-1/2}$ and the equatorial long Rossby wave speed becomes $-c_o\delta_{\text{art}}^{-1/2}/(2n + 1)$, $n = 1, 2, \cdots$. For $\delta_{\text{art}} > 1$, the wave speed is reduced; for $\delta_{\text{art}} < 1$, it is increased. Because of the square root dependence on δ_{art}, a quadrupling of the wave speed increases the computational cost by a factor of sixteen. (Although the limiting numerical criterion in the HGCM involves vertical mixing rather than wave speed, the required reduction of timestep with δ_{art} is essentially the same).

In the case of a modified shallow water model, such as Zebiak and Cane (1987), Battisti and Hirst (1988)

or the one presented in section 2, distorted physics experiments are even easier. The artificial factor, δ_{art}, should be introduced in front of the time derivative of the height equation, (55c), as well as (55a,b). The wave speed is increased proportional to δ_{art}^{-1}, instead of its square root and computational limitations are much less significant. Unfortunately, this option is not viable in a primitive equation model such as the HGCM, since there is not such a clear separation between the temperature equations that are involved in wave propagation and the temperature equations of the near-surface levels. It should be emphasized that changing the wave speed parameter in a modified shallow water model would be inferior to distorted physics experiments for testing the importance of wave time scales, since it would change the steady balance in presence of damping. For this reason, the use of δ_{art} provides the clearest *definition* of the fast-wave limit in realistic models, since it permits the rate of adjustment of the ocean to be changed in isolation from other effects.

The correspondence between distorted physics experiments and the scaling arguments of section 3 is straightforward. To see this most clearly in considering the slow SST mode derivation, simply rescale a slow time appropriate to its evolution using the small parameter δ of (24). Then all the time derivatives of the nondimensional shallow water equations (16–18) are multiplied by δ, relative to the time derivative term of the surface temperature equation (21) of the simple model. The artificial small parameter, δ_{art}, of the distorted physics experiments appears in an exactly analagous way, and "improves" the time scale separation between wave modes and the SST mode. Distorted physics experiments thus provide a rigorous way of defining the fast-wave limit which parallels the small parameter expansion used in the simple model case.

For the purpose of conducting distorted physics experiments in the HGCM, a case of slightly lower-than-standard coupling seems most appropriate as a control because of the simplicity of the evolution and because it may be hoped to avoid complex effects which might occur in a more highly nonlinear case. The numerical integration presented as Run-III in N is used. In this integration, the wind stress response of the atmospheric model was reduced. This had the effect of removing the coupled Kelvin wave secondary oscillations, thus permitting the ENSO-period oscillation to be seen more clearly, although at smaller amplitude than for the original parameter values. The evolution of SST anomalies along the equator over the first six years of this control run is presented for reference in Fig. 2. An initial wind stress perturbation in the western part of the basin initiates a growing unstable coupled mode that equilibrates into a periodic limit cycle of just over three year period. The westward propagation of anomalies is very clear during the cold phase. The warm phase begins with westward propagation of weak warm

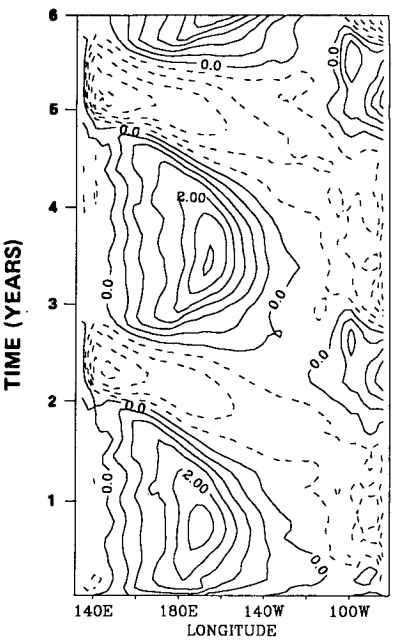

FIG. 2. Evolution of sea surface temperature anomalies along the equator over the first six years of the control run. Contour interval 0.5°C.

anomalies which follow in the wake of the cold anomalies. When the warm anomalies reach the central part of the basin, they grow in magnitude and the direction of propagation reverses, with the region of strongest anomalies moving back eastward into the eastern part of the basin.

The distorted-physics experiments are identical to the control, except for the introduction of δ_{art} into all momentum equations and the attendant reduction of timestep; $\delta_{art} = 1/4$ for the doubled wave speed experiment, and $\delta_{art} = 1/16$ for the quadrupled wave speed experiment. The runs are begun with a wind stress anomaly applied in the western Pacific over a period of one month, as for the control. In order to demonstrate the difference in wave speed between the control and the distorted-physics experiments, Fig. 3 shows the evolution of zonal current anomalies over the first six months of the control run (Fig. 3a), compared to doubled and quadrupled wave speed runs (Fig. 3b,c). The oceanic Kelvin wave packet excited by the initial wind stress anomaly may clearly be seen propagating eastward across the basin. The dominant phase speeds visible in the packet are characteristic of the first and second vertical modes, consistent with the results of ocean-only experiments. The increased rapidity of the adjustment process in the distorted-physics experiments may be clearly seen in these figures, occurring in weeks rather than months in the quadrupled wave speed case. The much more slowly evolving current anomalies which persist after the completion of

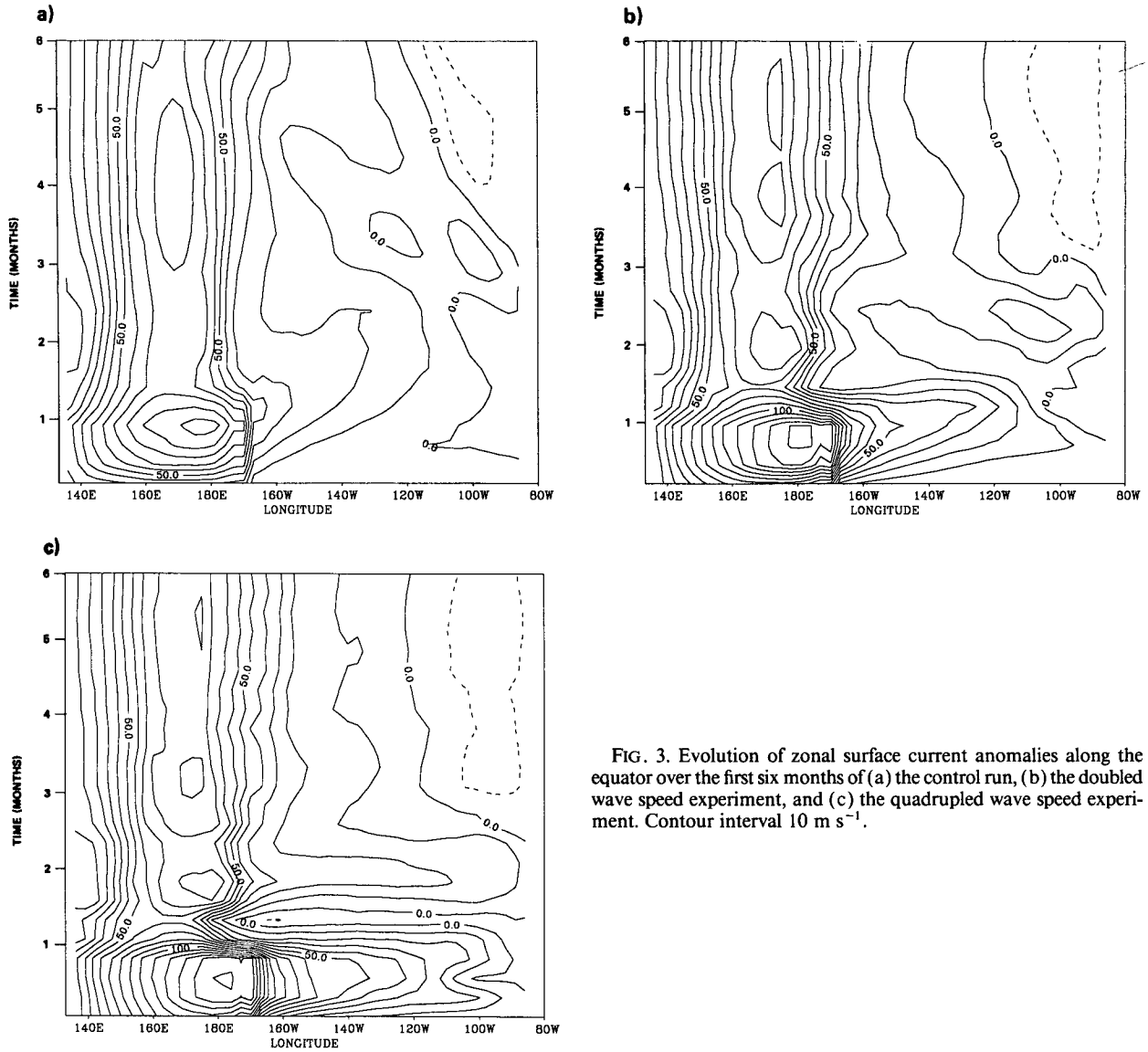

FIG. 3. Evolution of zonal surface current anomalies along the equator over the first six months of (a) the control run, (b) the doubled wave speed experiment, and (c) the quadrupled wave speed experiment. Contour interval 10 m s^{-1}.

the adjustment are due to the self-sustaining coupled oscillation and are changing on El Niño time scales.

The doubled wave speed experiment was integrated for six years, for which the SST anomaly evolution along the equator is shown in Fig. 4. The general form of the oscillation is clearly very much the same as the control, although the time scale is about 32 months instead of 37. This reduction is considerably less than one would expect if the time scale of propagation of information across the basin were the main factor in setting the period of the oscillation, considering that this has been cut in half.

The westward propagation of anomalies also appears slightly more pronounced in the doubled wave speed run than it was in the control. The mode looks more like a periodic-basin mode in which cold and warm anomalies succeed each other in a westward progression, the easterly wind stress to the east of each warm anomaly contributing to the maintenance of the following cold phase and vice versa. Furthermore, the time scale characteristic of the cold phase is not at all modified relative to the control. This tends to confirm the hypothesis that there is indeed an underlying phase speed, and therefore period, of the ENSO-period oscillation in the HGCM, which would exist even if the rate of information propagation across the basin were infinitely fast.

The doubled wave speed experiment alone would not be entirely conclusive since Battisti and Hirst (1988) find that the period of oscillation in the delayed

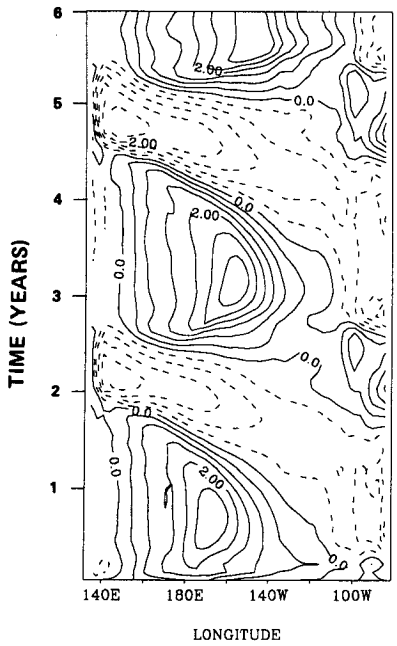

FIG. 4. As in Fig. 2, but for the doubled wave speed experiment.

oscillator can be considerably longer than twice the delay time due to wave propagation if the growth rate associated with the coupling is slow. Since there is a slight reduction in period between the control run and the doubled wave speed run, it is clear that the time scale of wave propagation does have some effect, although it does not appear to be of primary importance. In order to make these results more precise, the quadrupled wave speed run was carried out, the results from which may be seen in Fig. 5. The integration was limited to 4.5 years due to the computational costs, but this is enough to clearly establish the form and period of the oscillation. The evolution is remarkably similar to that of the doubled wave speed run, with a period which is shorter by only a half-month. It seems safe to extrapolate that this form and period would persist virtually unchanged in the limit of further wave speed increases.

These results serve to strongly confirm the hypothesis that slowly evolving coupled oscillations can exist even when the equatorial wave speed is so fast that the ocean comes into dynamical adjustment very quickly compared to the coupled evolution. Furthermore, the oscillations in the quadrupled wave speed experiment bear considerable resemblance to the oscillations in the control run, suggesting that, not only does the oscillation exist in the fast-wave limit, but this limit captures a significant part of the dynamics of the oscillation found at realistic parameter values.

However, the scaling analysis of section 3 suggested that, for a basin size of the Pacific, the fast-wave limit should be only marginally valid. It is relatively easy to carry out a further experiment to establish whether this is true by decreasing, instead of increasing, the wave speed. The results of a halved wave speed experiment are shown over six years in Fig. 6, again for SST anomaly along the equator. Other than using $\delta_{art} = 4$, this experiment is identical to the others. The oscillation is qualitatively the same, but is weaker, and the period has increased to closer to four years. This is consistent with what is expected from the simple model. As the wave speed becomes slower, the adjustment time scale becomes longer, and therefore more important. The weakening of the oscillation with slower wave speed suggests that the instability mechanism due to subsurface temperature perturbations associated with thermocline depth changes [term (B) of (53)] contributes significantly to the growth rate in the control case. As the wave speed slows, it takes longer for the slope of the thermocline to come into balance with the wind stress, thus making this term less effective in supporting the oscillation. This effect can thus be understood in terms of the fast-wave limit analysis. However, one might remark that the choice of control experiment was probably a fortunate one for obtaining such clean results. For stronger coupling, where nonlinearity begins to affect the period of the oscillation, the effect of the wave speed changes on the period might have been less clear.

These results are consistent with the suggestion, based on scaling analysis, that the fast wave limit does not strictly apply to the slow ENSO mode of the control run, but that this limit is nearby (in the sense that it can almost be obtained by a mere doubling of the wave

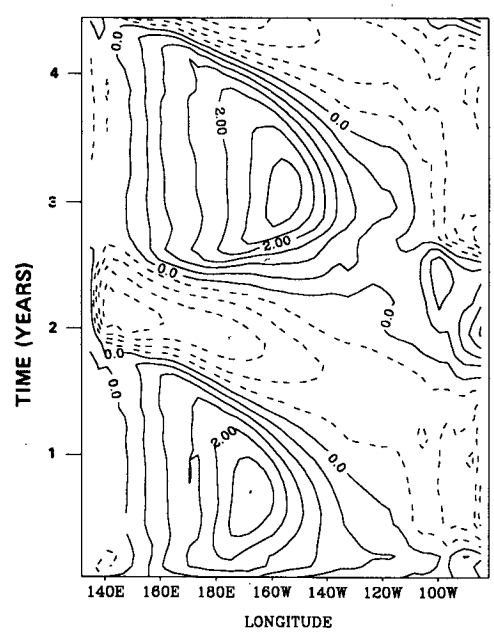

FIG. 5. As in Fig. 2, but over the 4.5 years of the quadrupled wave speed experiment.

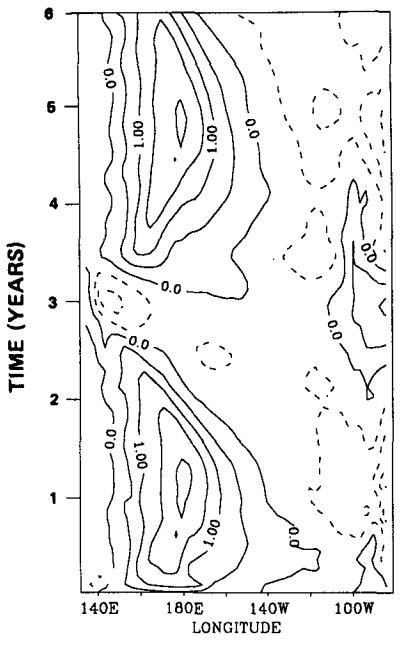

FIG. 6. As in Fig. 2, but for the halved wave speed experiment.

speed). Furthermore, the oscillation found in the fast-wave limit inherits the characteristics of the control oscillation to a large degree—certainly sufficiently for this limit to be a useful conceptual tool in discussing the oscillation.

It is also interesting to note that much of the asymmetry between the warm and cold phases found in the control run oscillation persist in the fast-wave limit. Although the discussion of the slow SST mode and fast-wave limit has been carried out in a linear context using constant coefficients for basic state values, it is interesting to speculate on why this might occur when nonlinear considerations are taken into account. During the warm phase, the upwelling is reduced or even shut off over a significant portion of the basin. Once the equatorial SST has warmed up to the temperature of the adjacent off equatorial regions, and the zonal gradient of SST has been flattened out over much of the basin, further changes in circulation can have only a relatively small effect on SST except in the remaining upwelling regions in the east. The evolution thus proceeds more slowly during the warm phase. In a realistic basic state, in which $\bar{w}$ is very small in the western part of the basin, this nonlinearity, represented by the upstream advection scheme in (1), enters even when the oscillation is near the bifurcation.

7. Conclusions and discussion

The scaling considerations presented in the context of a simple modified shallow-water model yield a number of asymptotic results useful for the discussion of tropical air–sea interaction. These analytic eigenvalue results have some degree of independence from the precise form of the atmospheric model. It is suggested that the eigenmode associated with the time derivative of the SST equation, termed the *SST mode*, is of fundamental importance to understanding interannual oscillations in coupled GCMs and in ENSO. In the limit when the equatorial wave speed is fast compared to time scales arising from the coupling, the SST mode appears as a slow eigenvalue which is independent of the faster wave-propagation time scales. In this *fast-wave limit*, the time scale of equatorial wave dynamics is unimportant to the oscillation, although thermocline perturbations in balance with the coupled wind stress anomalies can still play an important role. The scaling analysis suggests that the interannual oscillation observed in the hybrid coupled GCM exists at the boundary between the region of validity of the fast-wave limit and the region of parameter space where the slow SST mode becomes mixed with coupled versions of the traditional equatorial oceanic wave modes. Because of its simplicity, the fast-wave limit represents a useful conceptual tool. It clearly illustrates one extreme of the possible behavior of the coupled system, and shows in a simple context the manner in which several different mechanisms can all contribute to the growth rate of the ENSO unstable mode, while tending to cause propagation in different directions.

Asymptotic expressions are also obtained for coupled versions of the conventional equatorial ocean wave modes. These expressions are valid at low coupling whether or not the fast-wave limit applies, although their range of validity extends to higher coupling as the fast-wave limit is approached. In these modified ocean modes, multiple mechanisms also affect the coupling, but tend to oppose each other in causing growth and decay. This suggests that the instability of the SST mode, in which all mechanisms contribute to growth, should be much more robust to changes in parameters than instability of coupled ocean modes. However, the propagation characteristics of the SST mode, which is affected by coupling at zeroth order, will depend greatly on the balance of mechanisms supporting it in a particular model, while the oceanic modes retain their uncoupled form and frequency to a first approximation. The SST mode can propagate slowly eastward or westward, or remain stationary. The robustness of the instability and sensitivity of the characteristics of the SST mode suggest that interannual oscillations of this type might be found in many coupled models, but that the form and appearance of these oscillations may differ.

These results extend the numerical eigenvalue results of Hirst (1986) with regard to coupling of conventional wave modes, but differ significantly with regard to the SST mode. Important coupling mechanisms arise from inclusion of a surface mixed-layer, which strongly affects the SST mode. The equatorial-band approximation used in the current model is felt to be preferable

on physical grounds and avoids the high degree of degeneracy that arises at low coupling for analagous modes when SST tendency terms are parameterized uniformly in latitude. Asymptotic expressions for coupled Rossby and Kelvin modes may be used to reproduce several of the results of Hirst's model by dropping terms from the present model. However, the coupled Kelvin wave is suggested to be destabilized by a different mechanism, involving anomalous upwelling of mean vertical temperature gradient due to divergence in the shallow water component of the model. The coupled Kelvin wave behavior is consistent with the mode which arises in the HGCM as a secondary Hopf bifurcation. When mean upwelling is strong, the mode is stabilized by the term involving mean upwelling of subsurface temperature anomalies due to thermocline perturbations.

These results appear to be very different than those of Battisti and Hirst (1988), in which it is suggested that the Schopf and Suarez (1988) delayed oscillator mechanism can explain the time scale and other features of the oscillation in the Cane and Zebiak (1985) model. However, like the slow SST mode, the time variability in the delayed oscillator model is associated with the time derivative of the SST equation. If the form of the delayed oscillator equation is correct, then it is very reasonable to hypothesize that it must be related to the slow SST eigenmode. The fast-wave limit and the delayed oscillator may thus simply represent different extremes of the same mode.[2] In the HGCM, for the parameter values examined here, the interannual oscillation behaves very much as it does in the fast-wave limit, and cares relatively little about the time scale of wave reflections off the western boundary. If on the other hand, the coupling were cut off throughout much of the basin, as effectively occurs in the Cane and Zebiak model, the slow zonal propagation which gives rise to the period of the SST mode in the fast-wave limit would be inhibited, although it could still have a growth rate. Under these conditions it is very plausible that the linkage of the SST mode to oceanic wave modes which occurs at high coupling could become important to the existence of an oscillation. The tendency of the HGCM to couple across much of the basin, for the cases examined in N, is not necessarily the most realistic situation, although it does appear to characterize other coupled GCM results as well. The simplest characteristic that distinguishes the slow SST mode in the fast-wave limit from the delayed oscillator is the slow zonal propagation of SST anomalies in the former, versus growth of SST anomalies in place in the latter. Examples of both are found in observed SST time series.

The SST mode analysis presented here provides a simple framework in which some of the other recent coupled GCM results may be understood. Meehl (1990) finds westward-propagating coupled equatorial anomalies of interannual time scale in a global 5° latitude–longitude four-layer ocean GCM coupled to the NCAR R15 community climate model. Meehl notes that these modes appear to have little to do with equatorial wave propagation and have a close association between SST anomalies and westerly/easterly wind stress to the west of warm/cold SSTs producing upwelling anomalies. These anomalies can continue propagating from the Pacific into the Indian Ocean due to the existence of mean upwelling across both basins. There is little zonal SST gradient in the climatology. Similar slowly westward-propagating coupled anomalies are found in a coarse-resolution global ocean GCM coupled to the GFDL R15 atmospheric GCM, one of the two coupled GCMs described in Philander et al. (1989). In this case, advection of the mean vertical, zonal and meridional temperature gradients by perturbation currents all appear to be important during the onset phase of warm or cold periods. Both of these oscillations, exhibiting slow propagation of coherent atmospheric and oceanic anomalies and apparent lack of oceanic wave effects, appear to fit well into the slow SST mode hypothesis. In fact, the oscillation in these models most likely corresponds to the simplest version of the SST mode [given by (40) which requires fewer assumptions than the slightly more complicated version given by (53)] since the contribution of the thermocline depth anomalies is apparently not significant. The differences between the two models, in terms of which advection mechanisms dominate, is of secondary importance since all mechanisms contribute to the same mode. Whether advection by upwelling/meridional current anomalies or zonal current anomalies is more important to the instability makes relatively little difference to the evolution of the anomalies because both contribute in the same manner in the SST mode dispersion relationship.

The coupled phenomena described by Philander et al. (1989) in coupled model with a high resolution tropical Pacific Ocean component, on the other hand, appear to be much more difficult to understand in terms of the asymptotic results obtained here. The interannual warm and cold phases are generally of longer duration and what might be a secondary instability of roughly one year period complicates the evolution. The SST anomalies associated with the long period oscillation appear mainly to develop in place as a standing oscillation, although some eastward propagation may be noted. The main propagation tendency is seen in the subsurface heat content, which shows extremely slow eastward propagation. Although this propagation is too slow to be associated with any individual uncoupled ocean mode, it also fits poorly with the fast-

[2] Since the draft of this paper was first circulated, work with F.-F. Jin (Neelin et al. 1990) has indicated that this hypothesis is essentially correct—although the relationship of the SST mode to oceanic modes is more complex than the delayed oscillator equation would suggest—and work by A. Hirst (personal communication, 1990) suggests similar conclusions.

wave limit of the SST mode. However, as noted in the SST mode derivation, when the fast-wave limit fails, the SST eigenmode still exists but becomes mixed with the effects of the oceanic wave modes. It seems likely that to properly understand the results of the Philander et al. high-resolution model, an analysis of this more complex parameter regime is required, although this is difficult to carry out analytically.

The HGCM coupled experiment used here to demonstrate the applicability of the fast-wave limit apparently represents an intermediate region of parameter space in which the thermocline perturbation term in the SST equation is of similar importance to the perturbation current terms, but in which the fast-wave limit still applies. The dispersion relationship (53) for the SST mode in the fast-wave limit indicates that when the thermocline perturbation term increases in importance, it opposes the tendency to westward propagation due to the perturbation current terms. This may explain why the propagation of SST and associated anomalies is complex in the HGCM, with both westward and eastward propagation appearing during different periods, as well as stationary growth of anomalies during the warm phase. A balance between eastward and westward propagation tendencies will tend to create stationary growth of the SST mode, especially under the zonally inhomogeneous basic state conditions. The distorted physics experiments in the HGCM indicate that the low coupling control run is close to being well described by the fast-wave limit, but also that the region of parameter space where this fails is not far removed. These lend credence to the idea that relatively small differences between coupled models which affect the relative importance of thermocline versus advection processes (for instance, the sharpness of the vertical temperature gradient in the thermocline) and the effective coupling (for instance, if wind stress is deposited over a shallower layer) may lead between regimes in which the interannual oscillation is well represented by the SST mode in the fast-wave limit, and regimes in which the interaction of this mode and modes associated with wave dynamics must be considered.

While the fast-wave limit of the SST mode is intended to represent a useful idealization, the distorted physics method presented here provides a straightforward means of accessing this limit in almost any model for which sufficient computer resources are available. In the HGCM experiment in which it was tested, it proved to be a far better approximation than expected since the form and period of the oscillation were little changed as the equatorial wave speed was increased. Any model in which slow propagation of SST anomalies is observed is a reasonable candidate for testing the applicability of this limit. Whether the real ENSO cycle can be reasonably described in terms of the slow SST mode in the fast-wave limit or whether it is essential to treat the more complicated combination of the SST mode with wave effects—such as is represented by the delayed oscillator mechanism—must await further modeling results. In the interim, the robustness of the SST mode, in the sense that multiple mechanisms contribute to its growth and period, actually represents a major problem for ENSO simulation, since simulation of a sustained oscillation of interannual time scale does not guarantee that it is produced by the same mechanism or combination of mechanisms as the real system.

Acknowledgments. This work was supported by National Science Foundation Grant ATM-8905164. Enjoyable discussions with Gabriel Lau, David Battisti, Gerald Meehl, Paul Schopf, Mojib Latif, Ed Sarachik, Isaac Held, Michael Ghil, Mark Cane, Stephen Zebiak and, especially, George Philander and Anthony Hirst helped provide motivation for this analysis, encouragement and comments on the presentation. It is a pleasure to acknowledge discussions and further work with Fei-Fei Jin and Zheng Hao, and suggestions by the editor, Robert Gall, which influenced the revisions. Thanks to Clara Wong for assistance in typesetting the equations. Acknowledgment is made to the National Center for Atmospheric Research, which is sponsored by NSF, for computing time used in this research.

APPENDIX

Effects of Meridional Advection

The SST equation, (1), employs an equatorial strip approximation with first-order upstream-differencing in both vertical and meridional directions. When linearized about a state with mean upwelling and poleward meridional circulation, the upstream differencing implies that the meridional advection term does not appear explicitly, although its effects are implicitly present. In analysis of the contribution of various heat budget terms to the tendency of equatorial SST in coupled GCM experiments, however, the meridional advection terms will appear as important as the vertical advection terms due to the linkage of vertical and meridional circulation. A slightly more complicated treatment of the linearized SST equation is presented here to make it clear that advection due to the perturbation meridional currents may be treated implicitly in the vertical advection term for conceptual purposes.

Consider the perturbation SST equation for a narrow equatorial strip, as before, but in this case derived by averaging over a box of width L_y in the meridional direction with perturbation meridional currents and the basic state SST field assumed to have a fixed structure in y

$$v'(x, y) = v'_N(x)\nu(y)$$

$$\bar{T}(x, y) = \bar{T}(x) + \Delta T(x)\theta(y)$$

where $\nu(\pm L_y/2) = \pm 1$ and $\theta(\pm L_y/2) = 1$, $v'_N(x)$ is the perturbation meridional velocity at the north face of the box and $\Delta T(x) > 0$ is the temperature difference between the north and south faces of the box and the equator. The contribution of the $v'\bar{T}_y$ term to the time

tendency of y-averaged SST perturbations will be

$$-\overline{v'\bar{T}_y}^{y} = -v'_N(x)\frac{\Delta\bar{T}(x)}{(L_y/2)}M$$

where $\overline{(\ )}^{y}$ denotes meridional averaging over the box and

$$M = \overline{\nu(y)\frac{L_y}{2}\frac{d}{dy}\theta(y)}^{y}$$

is a nondimensional constant due to the assumed meridional structure. For the simplest case, when $\nu(y)$ is linear and $\theta(y)$ is quadratic, $M = 2/3$.

For the case $\nu(y)$ linear and w', u' constant within the box, the continuity equation (3) may be used without modification and for the SST mode we employ (48) and (49) for w' and u'. The contribution of the perturbation advection terms to the SST perturbation tendency thus becomes

$$\begin{aligned}\partial_t T' &= u'\bar{T}_x - w'\bar{T}_z - v'_N\frac{\Delta T}{L_y/2}M + \cdots \\ &= -b_u\bar{T}_x A_e(T') + b_w\left(\bar{T}_z + \frac{\Delta T}{H_1}M\right)A_e(T') \\ &\quad - H_1 B_u \bar{T}_z A_e(\bar{T}') + \cdots.\end{aligned}$$

It may be seen that the only effect of this treatment compared to simple upstream differencing is to modify the coefficient of one term, replacing $\bar{T}_z$ by $(\bar{T}_z + (\Delta T/H_1)M)$. This expression holds for zonally varying basic states; for the periodic basin case with zonally constant coefficients, the dispersion relation for the SST mode in the fast-wave limit is identical to (53) except for this modification to the coefficient in the term denoted A1 in Table 1, resulting in a slight increase in the strength of this term. No new physics is introduced, since this term in both cases measures the effects of advection by perturbations to the vertical–meridional circulation. The strength of this effect is increased in the present treatment because the meridional spreading of the SST anomaly produced by upwelling is taken into account explicitly.

For simple modeling purposes, the form of the SST equation used in (1) and (21) is preferred due to the simplicity and because the treatment considered in this Appendix is difficult to apply in the nonlinear case. The point demonstrated here is simply that, because advection by anomalous meridional circulation is effectively a slave to the corresponding vertical advection term, the latter may be used for conceptual purposes to represent both effects.

The role of mean meridional currents is to spread the SST anomaly produced by near-equatorial advection, as discussed by Battisti (1988). This effect is also treated implicitly in the equatorial strip model in the assumed y-structure of the atmospheric forcing. The results are insensitive to this structure, provided the meridional integral of the forcing of the atmosphere by SST is sufficiently large.

REFERENCES

Battisti, D. S., 1988: The dynamics and thermodynamics of a warming event in a coupled tropical atmosphere–ocean model. *J. Atmos. Sci.*, **45**, 2889–2919.

——, and A. C. Hirst, 1988: Interannual variability in the tropical atmosphere–ocean system: influence of the basic state and ocean geometry. *J. Atmos. Sci.*, **45**, 1687–1712.

Bender, C. M., and S. A. Orszag, 1978: *Advanced Mathematical Methods for Scientists and Engineers.* McGraw-Hill, 593 pp.

Bryan, K., and L. J. Lewis, 1979: A water mass model of the world ocean. *J. Geophys. Res.*, **84(C)**, 2503–2517.

Cane, M. A., 1979: The response of an equatorial ocean to simple wind stress patterns: I. Model formulation and analytic results. *J. Mar. Res.*, **37**, 233–252.

——, and S. E. Zebiak, 1985: A theory for El Niño and the Southern Oscillation. *Science*, **228**, 1084–1087.

Gill, A. E., 1980: Some simple solutions for heat induced tropical circulation. *Quart. J. Roy. Meteor. Soc.*, **106**, 447–462.

Harrison, D. E., 1989: Local and remote forcing of ENSO ocean waveguide response. *J. Phys. Oceanogr.*, **19**, 692–695.

Hirst, A. C., 1986: Unstable and damped equatorial modes in simple coupled ocean–atmosphere models. *J. Atmos. Sci.*, **43**, 606–630.

——, 1988: Slow instabilities in tropical ocean basin–global atmosphere models. *J. Atmos. Sci.*, **45**, 830–852.

Landau, L. D., and E. M. Lifshitz, 1965: Quantum Mechanics; Non-relativistic Theory. Pergamon, 616 pp.

Lindzen, R. S., and S. Nigam, 1987: On the role of sea surface temperature gradients in forcing low level winds and convergence in the tropics. *J. Atmos. Sci.*, **44**, 2240–2458.

Matsuno, T., 1966: Quasi-geostrophic motions in the equatorial area. *J. Meteor. Soc. Japan*, Ser.-II, **44**, 25–43.

McPhadden, M. J., and B. A. Taft, 1988: Dynamics of seasonal and intraseasonal variability in the Eastern Equatorial Pacific. *J. Phys. Oceanogr.*, **18**, 1713–1732.

Meehl, G. A., 1990: Seasonal cycle forcing of El Niño–Southern Oscillation in a global coupled ocean–atmosphere GCM. *J. Climate*, **3**, 72–98.

Nayfeh, A. H., 1973: *Perturbation Methods.* Wiley and Sons, 425 pp.

Neelin, J. D., 1988: A simple model for surface stress and low level flow in the tropical atmosphere driven by prescribed heating. *Quart. J. Roy. Meteor. Soc.*, **114**, 747–770.

——, 1989: A note on the interpretation of the Gill model. *J. Atmos. Sci.*, **46**, 2466–2468.

——, 1990: A hybrid coupled general circulation model for El Niño studies. *J. Atmos. Sci.*, **47**, 674–693.

——, and I. M. Held, 1987: Modeling tropical convergence based on the moist static energy budget. *Mon. Wea. Rev.*, **115**, 3–12.

——, F. -F. Jin and Z. Hao, 1990: Flow regimes of the tropical ocean–atmosphere system. *Proc. Int. TOGA Scientific Conference*, World Meteorological Organization, Technical Document, No. 379, WCRP-43, World Climate Research Programme, Geneva.

Philander, S. G. H., T. Yamagata and R. C. Pacanowski, 1984: Unstable air–sea interactions in the tropics. *J. Atmos. Sci.*, **41**, 604–613.

——, N. C. Lau, R. C. Pacanowski and M. J. Nath, 1989: Two different simulations of the Southern Oscillation and El Niño with coupled ocean–atmosphere general circulation models. *Phil. Trans. Roy. Soc. London*, **A329**, 167–178.

Schopf, P. S., and M. A. Cane, 1982: On equatorial dynamics, mixed layer physics and sea surface temperature. *J. Phys. Oceanogr.* **13**, 917–934.

——, and M. J. Suarez, 1988: Vacillations in a coupled ocean–atmosphere model. *J. Atmos. Sci.*, **45**, 549–566.

Sverdrup, H. U., 1947: Wind-driven currents in a baroclinic ocean with application to the equatorial currents in the eastern Pacific. *Proc. Natl. Acad. Sci.*, **33**, 318–326.

Zebiak, S. E., and M. A. Cane, 1987: A model ENSO. *Mon. Wea. Rev.*, **115**, 2262–2278.